

SUPPORTING INFORMATION

Identification of a RIP1 Kinase Inhibitor Clinical Candidate (GSK3145095) for the Treatment of Pancreatic Cancer

Philip A. Harris,^{*†} Jill M. Marinis,[†] John D. Lich,[†] Scott B. Berger,[†] Anirudh Chirala,[#] Julie A. Cox,[‡] Patrick M. Eidam,[†] Joshua N. Finger,[†] Peter J. Gough,[†] Jae U. Jeong,[†] James Kang,[†] Viera Kasparcova,[†] Lara K. Leister,[†] Mukesh K. Mahajan,[†] George Miller,^{#§} Rakesh Nagilla,[†] Michael T. Ouellette,[‡] Michael A. Reilly,[†] Alan R. Rendina,[‡] Elizabeth J. Rivera,[†] Helen H. Sun,[†] James H. Thorpe,[§] Rachel D. Totoritis,[‡] Wei Wang,[#] Dongling Wu,[#] Daohua Zhang,[†] John Bertin[†] and Robert W. Marquis[†]

[†]Pattern Recognition Receptor DPU and [‡]Platform Technology & Science, GlaxoSmithKline, Collegeville Road, Collegeville, Pennsylvania 19426, USA

[§] Platform Technology & Science, GlaxoSmithKline, Gunnels Wood Road, Stevenage, Hertfordshire SG1 2NY, UK

[#]S. Arthur Localio Laboratory, [§]Department of Cell Biology, New York University School of Medicine, 550 First Avenue, New York, NY 10016, USA

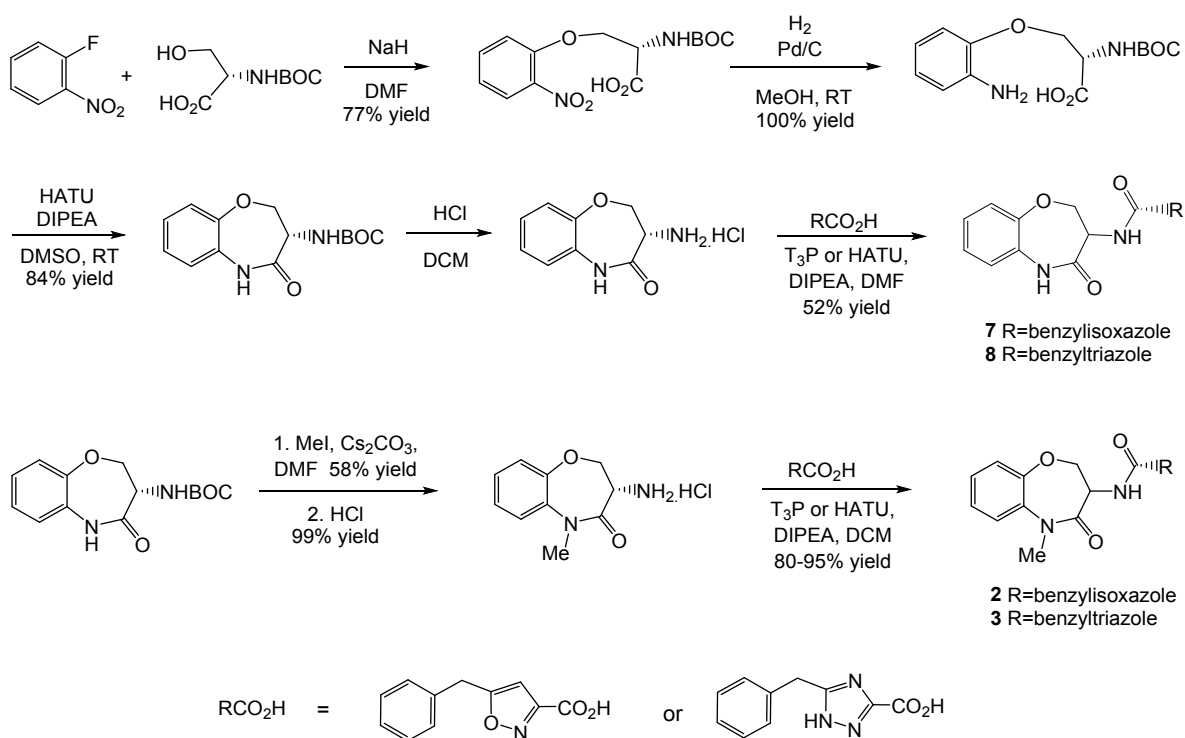
CONTENTS

- 1. Preparation of Compounds 2, 3, 6-11**
- 2. Enzyme preparation**
- 3. In vitro assays**
- 4. Mode of inhibition of Compound 6**
- 5. Compound 6 enzyme kinetics**
- 6. Compound 6 kinase selectivity and RIP1 species selectivity profiles**
- 7. Compound 6 RIP1 co-crystallization**
- 8. Compound 6: rat tissue distribution, permeability and P-gp substrate evaluation, hepatocyte turnover and human PK/PD predictions**
- 9. Additional PDOTS evaluation**
- 10. References**

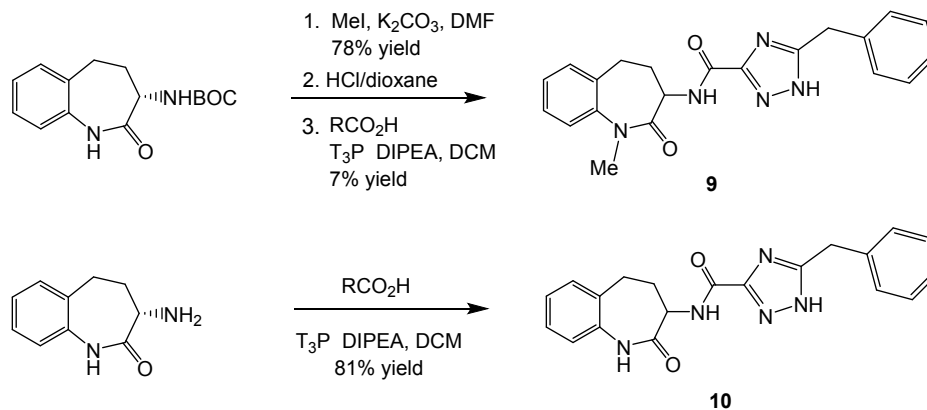
1. Preparation of Compounds 2, 3, 6-11

The route to prepare benzoxazepinones **2**, **3**, **7** and **8** has been described previously starting from BOC-L-serine and is detailed in Scheme 1.²² The unsubstituted (S)-3-amino-benzazepin-2-one is commercially available and can be converted to inhibitors **9** and **10** as shown in Scheme 2. The inhibitors **6** and **11** were obtained via 7,9-difluoro-benzazepin-2-one prepared starting from 6,8-difluoro-tetralone, conversion to the tosylate oxime and Beckmann rearrangement as outlined in Scheme 3. Conversion to the α -iodolactam, followed by displacement with azide and subsequent Staudinger reduction yielded the 3-amino-7,9-difluoro-benzazepin-2-one. The stereochemistry is set via a dynamic kinetic resolution using D-pyroglutamic acid and 3,5-dichlorosalicylaldehyde as catalyst. Coupling with 5-benzyl-triazole-3-carboxylic acid before or after methylation of the lactam nitrogen yielded **6** and **11**.

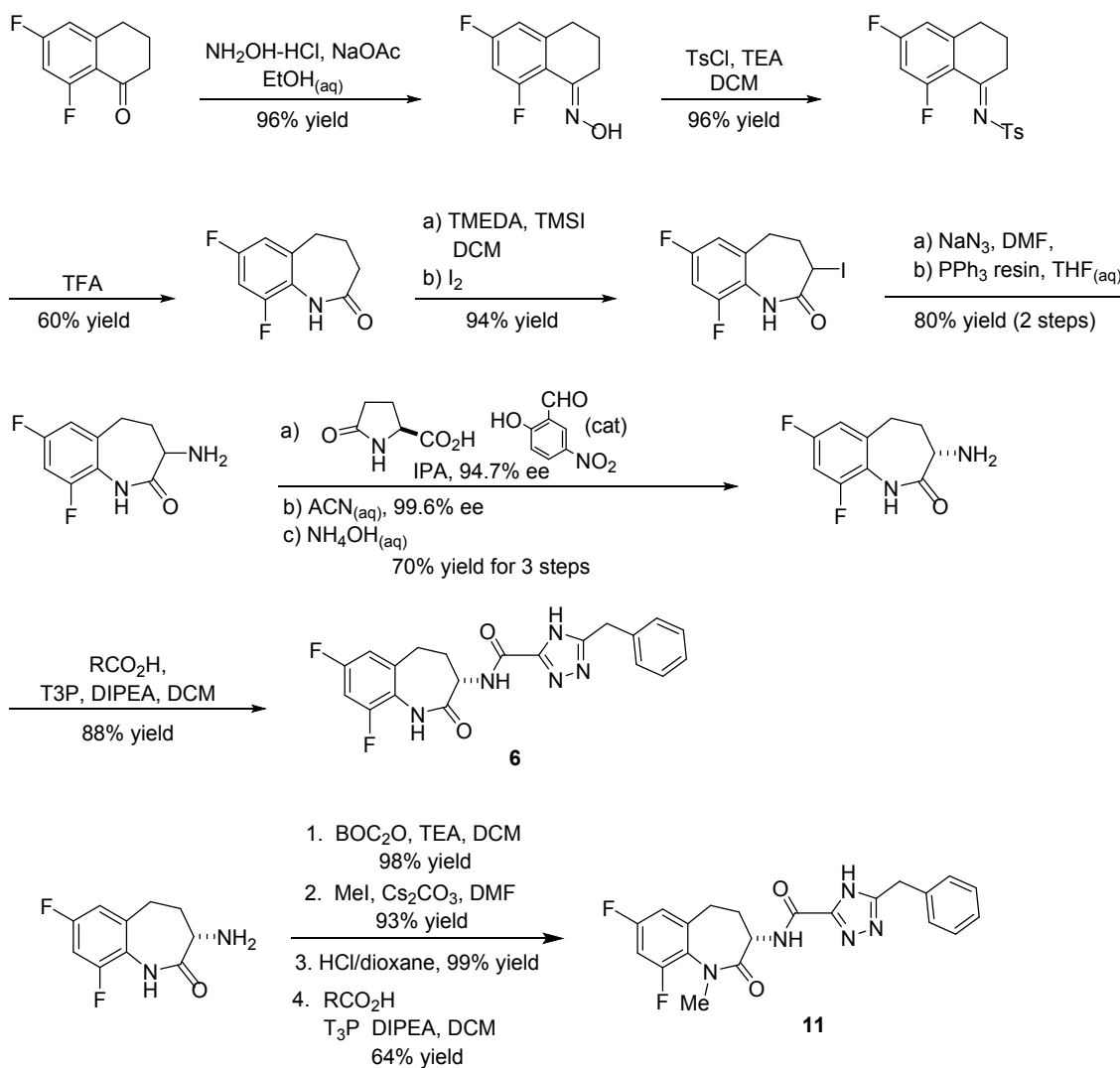
Scheme 1.



Scheme 2.



Scheme 3.



EXPERIMENTAL

General Methods. Unless otherwise noted, starting materials and reagents were purchased from commercial sources and used without further purification. Air or moisture sensitive reactions were carried out under a nitrogen atmosphere. Anhydrous solvents were obtained from Sigma-Aldrich. -Silica gel chromatography was performed using under standard techniques or using silica gel cartridges (RediSep normal phase disposable flash columns) on an Isco CombiFlash. Reverse phase HPLC purification was conducted on a Gilson HPLC (monitoring at a wavelength of 214 or 254 nm) with a YMC ODS-A C18 column (5 μ m, 75 mm 30 mm), eluting with 5-90% CH₃CN in H₂O with 0.1% TFA unless otherwise noted. ¹H NMR spectra were recorded on a Bruker Advance or Varian Unity 400 MHz spectrometer as solutions in DMSO-*d*₆ (unless otherwise stated). Chemical shifts (δ) are reported in ppm relative to an internal solvent reference. Apparent peak multiplicities are described as s (singlet), br s (broad singlet), d (doublet), dd (doublet of doublets), t (triplet), q (quartet), or m (multiplet). Coupling constants (J) are reported in hertz (Hz) after the integration.

Sciex LCMS analysis was performed on a PE Sciex Single Quadrupole 150EX, using a Thermo Hypersil Gold (C18, 20 x 2.1 mm, 1.9 μ particle diam.), 4-95% CH₃CN:H₂O (with 0.02% TFA) over 2 min., flow rate = 1.4 mL/min. at 55 °C. Waters LCMS was performed using the same column and conditions as for Sciex except using a Waters Acquity SQD UPLC/MS system. All tested compounds were determined to be \geq 95% purity by LCMS.

The following compounds were prepared as described previously: (*S*)-5-benzyl-*N*-(5-methyl-4-oxo-2,3,4,5-tetrahydrobenzo[b]-[1,4]oxazepin-3-yl)isoxazole-3-carboxamide (**2**), (*S*)-5-benzyl-*N*-(5-methyl-4-oxo-2,3,4,5-tetrahydrobenzo[b][1,4]oxazepin-3-yl)-4H-1,2,4-triazole-3-carboxamide (**3**) and (*S*)-5-benzyl-*N*-(4-oxo-2,3,4,5-tetrahydrobenzo[b][1,4]-oxazepin-3-yl)isoxazole-3-carboxamide (**7**).²²

The following intermediates were prepared as described previously: (*S*)-tert-butyl (4-oxo-2,3,4,5-tetrahydrobenzo[b][1,4]oxazepin-3-yl)carbamate, (*S*)-3-amino-2,3-dihydrobenzo[b][1,4]oxazepin-4(5H)-one hydrochloride, and 5-benzyl-4H-1,2,4-triazole-3-carboxylic acid.²²

The following intermediates are commercially available: (*S*)-3-amino-1,3,4,5-tetrahydro-2H-benzo[b]azepin-2-one, tert-butyl (*S*)-(2-oxo-2,3,4,5-tetrahydro-1H-benzo[b]azepin-3-yl)carbamate and 5-benzyl-3-isoxazolecarboxylic acid.

(*S*)-5-Benzyl-*N*-(7,9-difluoro-2-oxo-2,3,4,5-tetrahydro-1H-benzo[b]azepin-3-yl)-4H-1,2,4-triazole-3-carboxamide (6**).** To a solution of 6,8-difluoro-3,4-dihydronaphthalen-1(2H)-one (50 g, 274 mmol) in EtOH (500 mL) and water (167 mL) was added sodium acetate (33.8 g, 412 mmol) and hydroxylamine hydrochloride (28.6 g, 412 mmol). The reaction turned from a light pink to light yellow after hydroxylamine hydrochloride was added and a precipitate formed after 5 min. The reaction was stirred at rt for 150 min., after which water (500 mL) was added and the solids were filtered off and rinsed with water. The solid was dried to give (E)-6,8-difluoro-3,4-dihydronaphthalen-1(2H)-one oxime as an off-white solid (51.2 g). On sitting for 18 h, a small amount of additional product had precipitated from the filtrate. This was also filtered, washed with water and dried to give additional product (0.95 g). Total yield 52.15 g (96% yield). ¹H NMR (400 MHz, DMSO-*d*₆) δ ppm 1.71 (quin, *J*=6.38 Hz, 2 H), 2.60 - 2.84 (m, 4 H), 6.90 - 7.04 (m, 1 H), 7.09 (ddd, *J*=11.75, 9.35, 2.65 Hz, 1 H), 11.33 (s, 1 H). LCMS C₁₀H₉F₂NO (m/z): 198 (M+H⁺), >99% purity.

To a suspension of (E)-6,8-difluoro-3,4-dihydronaphthalen-1(2H)-one oxime (52.2 g, 265 mmol) in DCM (600 mL) was added TEA (55.3 mL, 397 mmol). The reaction was cooled in an ice water bath and p-toluenesulfonyl chloride (53 g, 278 mmol) added. The ice bath was

removed and the reaction stirred at rt for 22 h. The reaction solution was then washed with water (2 x 350 mL), 5% citric acid and brine. Concentration of the DCM solution resulted in an orange-tan solid which was dried to give (E)-6,8-difluoro-3,4-dihydronaphthalen-1(2H)-one O-tosyl oxime (92.1 g, 96% yield). ¹H NMR (400 MHz, DMSO-*d*₆) δ ppm 1.71 (quin, *J*=6.32 Hz, 2 H), 2.42 (s, 3 H), 2.75 (t, *J*=6.06 Hz, 2 H), 2.82 (t, *J*=6.57 Hz, 2 H), 7.05 - 7.13 (m, 1 H), 7.19 (ddd, *J*=11.49, 9.22, 2.53 Hz, 1 H), 7.48 (d, *J*=8.08 Hz, 2 H), 7.86 (d, *J*=8.34 Hz, 2 H). LCMS C₁₇H₁₅F₂NO₃S (m/z): 352 (M+H⁺), 98% purity.

Trifluoroacetic acid (220 mL) was added to (E)-6,8-difluoro-3,4-dihydronaphthalen-1(2H)-one O-tosyl oxime (92.1 g, 262 mmol) and the reaction mixture was stirred at 50 °C for 10 min. After 10 min the reaction was cooled in an ice/water bath and then quenched with cold water (1000 mL) over 5 min. The reaction mixture was stirred vigorously for 30 min in the ice bath and the resulting precipitate filtered off and washed with water. The crude product was stirred in 9:1 hexanes/Et₂O (500 mL), filtered off and resuspended in 3:1 hexanes/Et₂O (500 mL), filtered off and resuspended in Et₂O (250 mL). The resulting solid was filtered off, and dried in vacuum oven to give 7,9-difluoro-4,5-dihydro-1H-benzo[b]azepin-2(3H)-one (33.9 g, 60 % yield) as a light brown solid. ¹H NMR (400 MHz, DMSO-*d*₆) δ ppm 2.03 - 2.23 (m, 4 H), 2.73 (t, *J*=6.82 Hz, 2 H), 6.99 - 7.11 (m, 1 H), 7.20 (ddd, *J*=10.29, 9.16, 2.78 Hz, 1 H), 9.40 (s, 1 H). LCMS C₁₀H₉F₂NO (m/z): 198 (M+H⁺), 94% purity.

To a mixture of 7,9-difluoro-4,5-dihydro-1H-benzo[b]azepin-2(3H)-one (33.9 g, 172 mmol) in DCM (400 mL) cooled in an ice/water bath was added TMEDA (51.9 mL, 344 mmol), followed by TMSI (46.8 mL, 344 mmol) dropwise over 25 min. The light brown solution was stirred in the ice-bath for 60 min, and then iodine (65.4 g, 258 mmol) was added and mixture was stirred in the ice-bath for another 60 min. The reaction was quenched with aq. sodium thiosulfate, and stirred for 15 min. The resulting solid was filtered off, washed with water and DCM, and then dried in vacuum to give 7,9-difluoro-3-iodo-4,5-dihydro-1H-benzo[b]azepin-2(3H)-one (37.6 g, 66% yield) as a tan solid. The organic layer from the filtrate was separated and combined with DCM washes and this was washed with water and brine and concentrated. The resulting solid was triturated in 50 mL of ethyl acetate, filtered and dried to give additional product as an off-white solid (15.7 g, 28% yield). ¹H NMR (400 MHz, DMSO-*d*₆) δ ppm 2.53 - 2.65 (m, 1 H), 2.65 - 2.81 (m, 3 H), 4.61 - 4.76 (m, 1 H), 6.99 - 7.16 (m, 1 H), 7.16 - 7.33 (m, 1 H), 9.85 (s, 1 H). LCMS C₁₀H₈F₂INO (m/z): 324 (M+H⁺), >99% purity.

To 7,9-difluoro-3-iodo-4,5-dihydro-1H-benzo[b]azepin-2(3H)-one (53.2 g, 165 mmol) in DMF (400 mL) was added sodium azide (12.85 g, 198 mmol) and the mixture stirred at rt for 45 min. To the reaction was added ice-water (300 mL), then further diluted with water (500 mL) resulting in precipitation of a solid. The reaction was filtered to give 3-azido-7,9-difluoro-4,5-dihydro-1H-benzo[b]azepin-2(3H)-one as a tan solid. This was washed with water and used without further purification or drying. ¹H NMR (400 MHz, DMSO-*d*₆) δ ppm 2.03 - 2.21 (m, 1 H) 2.29 - 2.47 (m, 1 H) 2.73 - 2.85 (m, 2 H) 4.01 (dd, *J*=11.37, 8.08 Hz, 1 H) 7.10 (d, *J*=8.84 Hz, 1 H) 7.16 - 7.31 (m, 1 H) 9.98 (s, 1 H). LCMS (m/z): 239 (M+H⁺), 99% purity. To a solution of 3-azido-7,9-difluoro-4,5-dihydro-1H-benzo[b]azepin-2(3H)-one (direct from previous step) in THF (400 mL) was added water (2 mL) and PPh₃ resin (66 g, 3 mmol/g loading, 198 mmol). The reaction was stirred at rt for 24 h and then filtered through a small celite plug to remove the resin, rinsed with THF and the filtrate concentrated. The solid was triturated in Et₂O, filtered and dried to give 3-amino-7,9-difluoro-4,5-dihydro-1H-benzo[b]azepin-2(3H)-one (28.43 g, 80% yield over 2 steps) as an off-white solid. ¹H NMR (400 MHz, DMSO-*d*₆) δ ppm 1.76 (dtd, *J*=17.91, 6.46, 6.46, 2.78 Hz, 1 H), 2.14 - 2.35 (m, 1 H), 2.62 - 2.74 (m, 2 H), 3.15 (dd, *J*=11.49, 7.96 Hz, 1 H), 6.97 - 7.12 (m, 1 H), 7.20 (ddd, *J*=10.23, 9.22, 2.78 Hz, 1 H), 9.59 (br. s., 1 H). LCMS C₁₀H₁₀F₂N₂O (m/z): 213 (M+H⁺), >99% purity.

To a mechanically stirred solution of 3-amino-7,9-difluoro-4,5-dihydro-1H-benzo[b]azepin-2(3H)-one (28.4 g, 134 mmol) in iPrOH (1.25 L) at 70 °C was added 2-hydroxy-5-nitrobenzaldehyde (0.671 g, 4.02 mmol). Within 1 min, a thick precipitate formed. L-Pyroglutamic acid (17.28 g, 134 mmol) was added, the reaction mixture turned bright yellow, and was stirred at 70 °C for 5 days. The reaction was cooled to ~50 °C and the solid filtered off and washed twice with iPrOH. The solid was suspended in hexanes, stirred, filtered and dried to give 37.97 g of (S)-3-amino-7,9-difluoro-4,5-dihydro-1H-benzo[b]azepin-2(3H)-one L-pyroglutamate salt as an off-white solid. Chiral HPLC analysis using a Chiralpak IC analytical column (150 mm, 4.6 mm, 5u) eluting with 60:40 EtOH/hexanes (plus 0.1% diethylamine as modifier) as the mobile phase for 15 min. at 1 mL/min. provided good separation of a racemic standard. The R enantiomer eluted at 5.54 min. and the S enantiomer eluted at 6.32 min. This indicated that the chiral purity of the S enantiomer was 94.7% ee. This was suspended in 9:1 ACN:water (600 mL) and heated at 70 °C for 18 h. The suspension was cooled to ~40 °C, filtered, washed with CAN and dried to give 35.8 g of the salt as a white solid. Chiral HPLC analysis by the same method indicated that the chiral purity of the S enantiomer was >99% ee, with none of the R enantiomer detected. The salt was stirred vigorously in a mixture of conc. NH₄OH (15 mL) in water (200 mL) for 7 min. The solid was filtered, resuspended in a mixture of conc. NH₄OH (15 mL) in water (200 mL) for 7 min and filtered again. The solid was stirred in water (200 mL) for 15 min, filtered and dried to give (S)-3-amino-7,9-difluoro-4,5-dihydro-1H-benzo[b]azepin-2(3H)-one as a white solid (20 g, 70% yield). ¹H NMR (400 MHz, DMSO-*d*₆) δ ppm 1.68 - 1.84 (m, 1 H), 2.15 - 2.36 (m, 1 H), 2.57 - 2.81 (m, 2 H), 3.15 (dd, *J*=11.62, 7.83 Hz, 1 H), 7.07 (dd, *J*=8.84, 1.52 Hz, 1 H), 7.13 - 7.33 (m, 1 H), 9.59 (br. s., 1 H). LCMS C₁₀H₁₀F₂N₂O (m/z): 213 (M+H⁺), >99% purity.

To a mixture of (S)-3-amino-7,9-difluoro-4,5-dihydro-1H-benzo[b]azepin-2(3H)-one (19.1 g, 90 mmol), 5-benzyl-4H-1,2,4-triazole-3-carboxylic acid hydrochloride (22.65 g, 95 mmol) and DIEA (47.2 mL, 270 mmol) in DCM (650 mL) cooled in an ice/water bath was added 2,4,6-tripropyl-1,3,5,2,4,6-trioxatriphosphinane 2,4,6-trioxide (T3P, 50% by wt. in ethyl acetate) (81 mL, 135 mmol) dropwise over 13 min. The reaction was stirred at rt for 45 min becoming homogeneous after 10 min. The reaction was diluted with 0.5M HCl (600 mL) and a solid precipitated from the organic phase. The 2 layers were separated, the organics, including the solid, were treated with satd. NaHCO₃ solution and the 2 phases shaken vigorously. The 2 layers were separated and the solid filtered off and washed with DCM. The solid was stirred in water (600 mL) for 60 min, filtered, and washed with water, and dried in vacuum oven at 50 °C to give 33.1 g of product. The solid was resuspended in water (700 mL) and stirred for 2 h. The solid was filtered, washed with water, and dried in vacuum oven at 50 °C to give (S)-5-benzyl-N-(7,9-difluoro-2-oxo-2,3,4,5-tetrahydro-1H-benzo[b]azepin-3-yl)-4H-1,2,4-triazole-3-carboxamide (**6**) as a white solid (32 g, 88% yield). ¹H NMR (400 MHz, DMSO-*d*₆) δ ppm 2.26 (br. s., 1 H), 2.35 - 2.48 (m, 1 H), 2.67 - 2.89 (m, 2 H), 4.12 (br. s., 2 H), 4.34 (dt, *J*=11.43, 7.93 Hz, 1 H), 7.15 (d, *J*=8.84 Hz, 1 H), 7.19 - 7.47 (m, 6 H), 8.22 (br. s., 1 H), 9.96 (s, 1 H), 14.31 (br. s., 1 H). LCMS C₂₀H₁₇F₂N₅O₂ (m/z): 313 (M+Na⁺), 398 (M+H⁺), >99% purity. Chiral HPLC analysis using a ChromegaChiral™ CC4 analytical column (150 mm, 4.6 mm, 5u) eluting with CH₃CN (plus 0.2% formic acid and 0.1% diethylamine as modifiers) as the mobile phase for 30 min. at 1 mL/min. provided good separation of a racemic standard. The R enantiomer eluted at 4.57 min. and the S enantiomer (**6**) eluted at 5.96 min. This indicated that the chiral purity of **6** prepared by this method was >99.9% ee, with none of the R enantiomer detected. Anal. Calcd for C₂₀H₁₇F₂N₅O₂ C, 60.43; H, 4.31; N, 17.63. Found: C, 60.33; H, 4.03; N, 17.00.

(S)-5-Benzyl-N-(4-oxo-2,3,4,5-tetrahydrobenzo[b][1,4]oxazepin-3-yl)-4H-1,2,4-triazole-3-carboxamide (8). To a mixture of (S)-3-amino-2,3-dihydrobenzo[b][1,4]oxazepin-4(5H)-one hydrochloride (1.024 g, 4.77 mmol) and 5-benzyl-4H-1,2,4-triazole-3-carboxylic acid hydrochloride (1.2 g, 5.0 mmol) in DCM (30 mL) was added DIPEA (9.5 mL, 54.6 mmol) and the resulting solution stirred at rt for 1 hour. T₃P solution (50% by wt. in EtOAc, 4.27 mL, 7.16 mmol) was added and the reaction stirred at rt for a further 1 hour. Additional T₃P solution (1 mL, 1.68 mmol) and DIEA (1 mL, 5.74 mmol) were added and the reaction stirred at rt for a further 1 hour. The reaction was concentrated on a rotavapor to remove DCM, then redissolved in EtOAc and washed with 1M HCl, satd. NaHCO₃, water and brine. The organic layer was concentrated to a foam which was redissolved in EtOAc (10 mL) and stirred at rt for 3 days to give a thick paste. Added more EtOAc (15 mL) and stirred vigorously for 10 min. The resulting solid was filtered off and washed with EtOAc. The filtrate was concentrated and purified by silica gel chromatography (24 g silica column; 10-65% EtOAc/hexanes). The filtered solid and the purified fractions from chromatography were combined and dried to give (S)-5-benzyl-N-(4-oxo-2,3,4,5-tetrahydrobenzo[b][1,4]oxazepin-3-yl)-4H-1,2,4-triazole-3-carboxamide (**8**) as an off-white solid (0.905 g, 52% yield). ¹H NMR (400 MHz, DMSO-*d*₆) δ ppm 4.05 - 4.20 (m, 2 H), 4.43 (dd, *J*=10.52, 6.46 Hz, 1 H), 4.52 (t, *J*=10.52 Hz, 1 H), 4.80 (dt, *J*=10.65, 7.22 Hz, 1 H), 7.04 - 7.19 (m, 4 H), 7.19 - 7.45 (m, 7 H), 8.55 (br. s., 1 H), 10.12 - 10.25 (m, 1 H). LCMS C₁₉H₁₇N₅O₃ (m/z): 364 (M+H⁺), >99% purity.

(S)-5-Benzyl-N-(1-methyl-2-oxo-2,3,4,5-tetrahydro-1H-benzo[b]azepin-3-yl)-4H-1,2,4-triazole-3-carboxamide (9). To (S)-tert-butyl (2-oxo-2,3,4,5-tetrahydro-1H-benzo[b]azepin-3-yl)carbamate (300 mg, 1.09 mmol) dissolved in DMF (4 mL) was added MeI (0.081 mL, 1.3 mmol). Potassium carbonate (210 mg, 1.52 mmol) was then added portion wise. After stirring for 2 days at rt, the reaction was quenched with water (20 mL) and stirred for 15 min. The resulting solid was filtered off, washed with water and dried to afford (S)-tert-butyl (1-methyl-2-oxo-2,3,4,5-tetrahydro-1H-benzo[b]azepin-3-yl)carbamate (246 mg, 78 % yield). ¹H NMR (400 MHz, DMSO-*d*₆) δ ppm 1.33 (s, 9 H), 1.91 - 2.20 (m, 2 H), 2.57 - 2.72 (m, 2 H), 3.27 (s, 3H), 3.86 (dt, *J*=11.68, 8.31 Hz, 1 H), 7.02 (d, *J*=8.59 Hz, 1 H), 7.15 - 7.25 (m, 1 H), 7.29 (d, *J*=7.07 Hz, 1 H), 7.32 - 7.42 (m, 2 H). LCMS C₁₆H₂₂N₂O₃ (m/z): 313 (M+Na⁺), 291 (M+H⁺), >99% purity.

To a solution of (S)-tert-butyl (1-methyl-2-oxo-2,3,4,5-tetrahydro-1H-benzo[b]azepin-3-yl)carbamate (240 mg, 0.83 mmol) in DCM (5 mL) was added 4N HCl in dioxane (0.827 mL, 3.31 mmol) and the reaction stirred at rt for 3h. Additional 4N HCl was added (0.205 mL, 0.83 mmol). And stirring continued for 24h. The reaction was concentrated to afford (S)-3-amino-1-methyl-4,5-dihydro-1H-benzo[b]azepin-2(3H)-one hydrochloride (270 mg, 144 % yield) which was used directly in the next step. ¹H NMR (400 MHz, DMSO-*d*₆) δ ppm 2.07 - 2.18 (m, 1 H), 2.36 - 2.49 (m, 1 H), 2.64 - 2.85 (m, 2 H), 3.28 - 3.35 (s, 3 H), 3.59 - 3.73 (m, 1 H), 7.21 - 7.32 (m, 1 H), 7.33 - 7.39 (m, 1 H), 7.39 - 7.45 (m, 2 H), 8.28 (br. s., 3 H). LCMS C₁₁H₁₄N₂O (m/z): 191 (M+H⁺), 96% purity.

To a solution of (S)-3-amino-1-methyl-4,5-dihydro-1H-benzo[b]azepin-2(3H)-one hydrochloride (270 mg, 1.2 mmol), 5-benzyl-4H-1,2,4-triazole-3-carboxylic acid (290 mg, 1.43 mmol) and DIPEA (0.832 mL, 4.76 mmol) in DCM (6.5 mL) was added T₃P solution (50% by wt. in EtOAc, 1.2 mL, 2.03 mmol). The reaction was stirred at rt for 90 min. and then quenched with EtOAc and water. The aqueous layer was separated and extracted with further with EtOAc and the combined organic extracts were purified via silica gel chromatography eluting with 5-60% (EtOH/EtOAc 3:1)/heptane. The desired fractions were concentrated to afford (S)-5-benzyl-N-(1-methyl-2-oxo-2,3,4,5-tetrahydro-1H-benzo[b]azepin-3-yl)-4H-1,2,4-triazole-3-carboxamide (**9**) (33 mg, 7 % yield). ¹H NMR (400 MHz, CDCl₃) δ ppm 1.97

- 2.17 (m, 1 H), 2.57 - 2.82 (m, 2 H), 2.82 - 3.01 (m, 1 H), 3.44 (s, 3 H), 4.21 (s, 2 H), 4.64 (dt, $J=11.12, 7.58$ Hz, 1 H), 7.18 - 7.27 (m, 3 H) 7.30 - 7.38 (m, 6 H), 8.19 (d, $J=7.83$ Hz, 1 H). LCMS $C_{21}H_{21}N_5O_2$ (m/z): 376 (M+H⁺), >99% purity.

(S)-5-Benzyl-N-(2-oxo-2,3,4,5-tetrahydro-1H-benzo[b]azepin-3-yl)-4H-1,2,4-triazole-3-carboxamide (10). To a suspension of (S)-3-amino-4,5-dihydro-1H-benzo[b]azepin-2(3H)-one (1.0 g, 5.67 mmol) and 5-benzyl-4H-1,2,4-triazole-3-carboxylic acid hydrochloride (1.5 g, 6.24 mmol) in DCM (48.5 mL) at 0 °C was added DIPEA (3.47 mL, 19.9 mmol). After stirring for 30 min at 0 °C, T₃P solution (50% by wt. in EtOAc, 4.74 mL, 7.94 mmol) was slowly added. After stirring for 20 min at 0 °C, the reaction solution was warmed up to rt. After 5 h, additional DIPEA (0.5 mL) and T₃P solution (0.5 mL) were added and the reaction stirred overnight at rt. The resultant solid was collected by filtration and washed with DCM and dried to give product (464 mg, 22 % yield) as a white solid. The filtrate was concentrated and stirred in water to precipitate a white solid. The solid was collected and washed with water and Et₂O and dried to give additional product (1.22 g, 59 % yield). Combining products gave (S)-5-benzyl-N-(2-oxo-2,3,4,5-tetrahydro-1H-benzo[b]azepin-3-yl)-4H-1,2,4-triazole-3-carboxamide (**10**) (1.68 g, 81 % yield). ¹H NMR (400 MHz, DMSO-*d*₆) δ ppm 2.23 (d, $J=9.09$ Hz, 1 H), 2.34 - 2.49 (m, 1 H), 2.63 - 2.89 (m, 2 H), 4.11 (s, 2 H), 4.33 (dt, $J=11.62, 7.83$ Hz, 1 H), 7.04 (d, $J=7.83$ Hz, 1 H), 7.09 - 7.20 (m, 1 H), 7.20 - 7.40 (m, 7 H), 8.28 (br. s., 1 H), 10.01 (s, 1 H), 14.41 (br. s., 1 H). LCMS $C_{20}H_{19}N_5O_2$ (m/z): 362 (M+H⁺), >99% purity.

(S)-5-Benzyl-N-(7,9-difluoro-1-methyl-2-oxo-2,3,4,5-tetrahydro-1H-benzo[b]azepin-3-yl)-4H-1,2,4-triazole-3-carboxamide (11). To a solution of (S)-3-amino-7,9-difluoro-4,5-dihydro-1H-benzo[b]azepin-2(3H)-one (1.1 g, 5.18 mmol) and TEA (1.084 mL, 7.78 mmol) in DCM (10 mL) stirred under N₂ at 20 °C was added Boc₂O (1.32 mL, 5.70 mmol) dropwise over 5 min. The reaction mixture was stirred at rt for 2 h and then diluted with DCM (30mL) and this was washed with water (4 x 10mL), the organic phase was separated and washed with brine, dried over Na₂SO₄, filtered and concentrated to afford (S)-tert-butyl (S)-tert-butyl (7,9-difluoro-2-oxo-2,3,4,5-tetrahydro-1H-benzo[b]azepin-3-yl)carbamate (1.6 g, 98 % yield) as a cream colored solid. ¹H NMR (400 MHz, DMSO-*d*₆) δ ppm 1.35 (s, 9 H), 2.02 - 2.30 (m, 2 H), 2.62 - 2.83 (m, 2 H), 3.83-3.91 (m, 1 H), 7.02-7.07 (m, 2 H), 7.22 - 7.36 (m, 1 H), 9.63 (s, 1 H). LCMS $C_{19}H_{26}F_2N_2O_3$ (m/z): 213 ([M-BOC]+H⁺), 99% purity.

To a mixture of cesium carbonate (2.337 g, 7.17 mmol) and (S)-tert-butyl (7,9-difluoro-2-oxo-2,3,4,5-tetrahydro-1H-benzo[b]azepin-3-yl)carbamate (1.6 g, 5.12 mmol) in DMF (25 mL) was added iodomethane (0.384 mL, 6.15 mmol). The reaction was stirred at room temperature for 25 min. and then quenched with water (25 mL) and stirred vigorously for a further 5 min. The resulting solid was filtered off, rinsed with water and then hexane and dried to give (S)-tert-butyl (7,9-difluoro-1-methyl-2-oxo-2,3,4,5-tetrahydro-1H-benzo[b]azepin-3-yl)carbamate (1.6 g, 93% yield). ¹H NMR (400 MHz, DMSO-*d*₆) δ ppm 1.30 (s, 9 H), 1.95 - 2.20 (m, 2 H), 2.60 - 2.80 (m, 2 H), 3.20 (s, 3H), 3.81-3.90 (m, 1 H), 7.13-7.20 (m, 2 H), 7.28 - 7.41 (m, 1 H). LCMS $C_{16}H_{20}F_2N_2O_3$ (m/z): 227 ([M-BOC]+H⁺), 97% purity.

To a solution of (S)-tert-butyl (7,9-difluoro-1-methyl-2-oxo-2,3,4,5-tetrahydro-1Hbenzo[b]azepin-3-yl)carbamate (1.6 g, 4.9 mmol) in DCM (5 mL) stirred at 0 °C was added 4M HCl in 1,4-dioxane (2.45 mL, 9.81 mmol) and the reaction stirred at rt for 2h. The reaction mixture was concentrated under the reduced pressure and the solid obtained was triturated in Et₂O and dried to obtain (S)-3-amino-7,9-difluoro-1-methyl-4,5-dihydro-1H-benzo[b]azepin-2(3H)-one hydrochloride (1.3 g, 99 % yield) as an off white solid. ¹H NMR (400 MHz, DMSO-*d*₆) δ ppm 2.02 - 2.20 (m, 1 H), 2.30 - 2.48 (m, 1 H), 2.74 - 2.85 (m, 2 H), 3.24 (s, 3H), 3.81-

3.89 (m, 1 H), 7.18-7.22 (m, 1 H), 7.38-7.42 (m, 1 H), 8.40 (br. s., 3 H). LCMS C₁₁H₁₃ClF₂N₂O (m/z): 227 ([M+H⁺]), 98% purity.

A mixture of (S)-3-amino-7,9-difluoro-1-methyl-4,5-dihydro-1H-benzo[b]azepin-2(3H)-one hydrochloride (0.04 g, 0.152 mmol), 5-benzyl-4H-1,2,4-triazole-3-carboxylic acid hydrochloride (0.038 g, 0.16 mmol) and DIPEA (0.093 mL, 0.533 mmol) in DCM (2 mL) was stirred vigorously for 5 min. A solution of T₃P (50% by wt. in EtOAc, 0.127 mL, 0.213 mmol) was added and the reaction stirred at rt for 10 min. The reaction was diluted with EtOAc and washed with 1M HCl solution, satd. NaHCO₃ followed by brine. The organic phase was concentrated to give a solid which was suspended in hexanes, filtered and dried to give (S)-5-benzyl-N-(7,9-difluoro-1-methyl-2-oxo-2,3,4,5-tetrahydro-1H-benzo[b]azepin-3-yl)-4H-1,2,4-triazole-3-carboxamide (**11**) (41 mg, 64 % yield) as a white solid. ¹H NMR (DMSO-d₆) δ 2.16 - 2.37 (m, 2H), 2.70 - 2.82, (m, 2H), 4.11 (s, 2H), 3.20 (s, 3H), 4.35 (dt, J = 10.9, 8.0 Hz, 1H), 7.14 - 7.42 (m, 7H), 8.33 (br. m., 1H), 14.52 (br. s., 1H). LCMS C₂₁H₁₉F₂N₅O₂ (m/z): 412 (M+H⁺), >99% purity.

2. RIP1 (1-375) preparation

The human RIP1 gene [receptor (TNFRSF)-interacting serine-threonine kinase 1] was cloned from human adrenal gland cDNA. Primers were designed from the reference sequence NM_003804.3 using the 5' Kozak-adapted gene-specific primer and the 3' gene-specific primer. PCR products were cloned into the pENTR/TEV/D-TOPO vector. The Gateway LR reaction was performed with a pDEST8HisGSTTev vector to produce the final clone: pDEST8HisGSTTev human RIPK1 1 375. Baculovirus was generated using the bac to bac system (Invitrogen) according to manufacturer's specifications. pDEST8HisGSTTev human RIPK1 1 375 baculovirus infected insect cells (BII-Cs) were prepared during baculovirus generation according to [Wasilko and Lee, 2006]. RIP1 protein was purified by capture on Glutathione Agarose (Pierce) and eluted with 20 mM reduced glutathione. The protein was then run on a size exclusion column (Superdex200, GE Healthcare) to separate the aggregated protein from the active dimeric protein and to exchange the protein into assay compatible buffer (25 mM Tris, pH7.5, 150 mM NaCl, 1 mM DTT, 5% Glycerol). The human RIP1 crystallography construct was Flag.1-294, C34A, C127A, C233A, C240A. Similar protocols were used to generate the the orthologs; mouse RIP 1(1-378), rat RIP1(1-377), rabbit RIP1 (1-371), dog RIP1 (1-373), minipig RIP1 (1-375), and monkey RIP1 (1-379).

3. In vitro assays

ADP-Glo Activity Assay. The catalytic activity of RIP1 was quantified utilizing the Promega ADP-Glo kinase kit as previously described (Harris et al, 2016) using either a four-parameter curve fit or a tight binding curve fit for compounds whose potency was less than the detection limit of the assay (~ half the enzyme concentration). Data are presented as the mean IC₅₀ from at least n=2 determinations.

U937 and L929 Cell Necroptosis Assays. The efficacy of RIP1 inhibitors were determined in vitro using human monocytic leukemia U937 cells or mouse L-cells NCTC 929 (L929) cells in a necroptosis assay as previously described (Harris et al, 2016).

Biological in Vitro Whole Blood Assay. Compound **6** was evaluated in human and cynomolgus monkey whole blood assays. For the assay, 3 stock solutions each of 200 ng/mL TNF (Cell

Sciences), 400 μ M QVD-Oph or zVAD.fmk (R&D Systems) and 20 μ M SMAC mimetic 2',2'''-(2,4-hexadiyne-1,6-diyl)bis[1-[[[(2S)-1-(N-methyl-L-alanyl-L-threonyl)-2-pyrrolidinyl]methyl]-5-(phenylthio)-1H-tetrazole (RMT 5265, Li et al, 2004) were prepared in phenol red free RPMI 1640 medium supplemented with 1% fetal bovine serum, 100 units/mL penicillin and 100 μ g/mL streptomycin. In addition, 5-fold dilution series of compound **6** were prepared in the same medium supplemented with 1% DMSO, with top concentrations of 1 μ M and 5 μ M for human and monkey assays, respectively. A 5 μ L solution of compound **6** at each dilution was transferred to a 96 well tissue culture treated assay plate and 5 μ L of each of the 3 stock solutions was added. Whole blood was collected by venous puncture in heparin tubes (Griener Bio-One). Whole blood (80 μ L) was added to each well of the assay plate, mixed briefly and incubated for 6 h at 37 °C, 5% CO₂. Following incubation, PBS (200 μ L) was added to each well and the assay plate was centrifuged at 1700 rpm for 5 min. Supernatants were frozen at -70°C. Concentrations of MIP-1 β (human) and IL-1 β (monkey) were determined by sandwich ELISA (Meso Scale Discovery) following the manufacturer's instructions.

Neutrophil Necroptotic Assay. Compound **6** was evaluated in human neutrophils isolated from whole blood using standard method involving dextran sedimentation and Ficoll-Hypaque density gradient centrifugation. Necroptotic cell death was induced in freshly isolated neutrophils with 10 ng/ml TNF α , 50 μ M QVD-Oph and 100 nM SMAC mimetic 2',2'''-(2,4-hexadiyne-1,6-diyl)bis[1-[[[(2S)-1-(N-methyl-L-alanyl-L-threonyl)-2-pyrrolidinyl]methyl]-5-(phenylthio)-1H-tetrazole (SMAC mimetic RMT 5265, Li et al, 2004). Induced cell death was evaluated 21 h post stimulation by measuring cellular ATP levels and LDH release into media. Intracellular ATP levels were quantified using CellTiter-Glo Luminescent Cell Viability assay (Promega). Lactate dehydrogenase (LDH) release into media was evaluated using a Cytotoxicity Detection kit [LDH] (Roche Applied Sciences). Concentration of MIP-1 β in cell-free supernatants was determined by sandwich ELISA (Meso Scale Discovery) following the manufacturer's instructions.

4. Mode of inhibition of Compound **6**

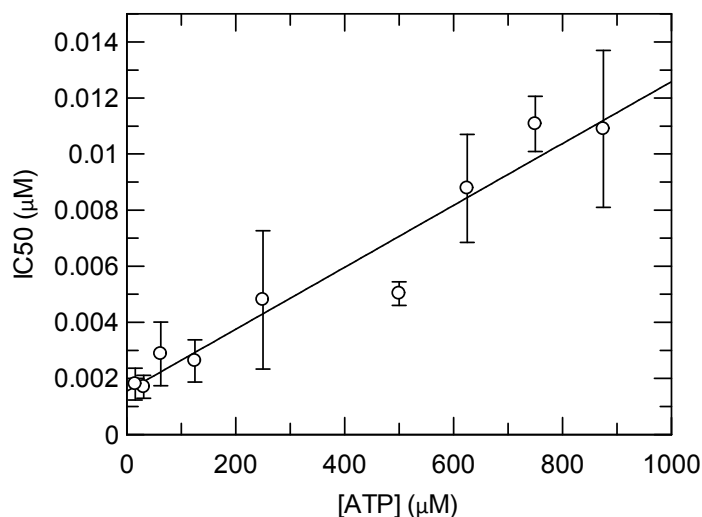
To determine the mode of inhibition of Compound **6** on hRIP1 (1-375), the effect of substrate concentration on the IC₅₀ was determined using an ADP-Glo assay measuring the activity of RIP1 by quantifying the conversion of ATP to ADP due to both enzyme catalyzed autophosphorylation and ATPase activities. Test compound was prepared in assay buffer (50 mM Hepes pH 7.5, 50 mM NaCl, 30 mM MgCl₂, 1 mM DTT, 0.02% CHAPS, 0.5 mg/mL BSA) and serially diluted 1:1.5 in a 22 point titration (high final concentration 3 μ M) and added to a 384 white low volume Greiner plate. 3.5 μ L of each inhibitor concentration and 3.5 μ L of 25 nM enzyme (final) in assay buffer were added to the plate. Following these additions, 3.5 μ L of ATP (15.6 μ M to 875 μ M final) in assay buffer was added to the plate to initiate the reaction. The reaction progressed for 5h at room temperature. Following this reaction 5 μ L of Promega ADP-Glo Reagent with 0.02% CHAPS was added to each well and incubated for 1h at room temperature. This quenched the kinase reaction and depleted any remaining ATP. 5 μ L of Promega ADP-Glo Detection solution with 0.02% CHAPS was then added to each well and incubated at room temperature for 30 min. This converted ADP to ATP and introduced luciferase and luciferin to detect ATP, allowing for the quantification of the ADP produced by RIP1. The luminescence was then measured on a Perkin Elmer ViewLux. Luminescence data was normalized to the high and low controls for each ATP concentration and expressed as fractional activity remaining. The IC₅₀ at each ATP concentration was determined using the Morrison tight binding equation (eq 1). IC₅₀ values were then plotted as a function of substrate concentration (S) using the competitive inhibition equation (eq 2) where K_i

is the inhibition constant and K_m is the Michaelis constant for S [Williams and Morrison, 1979].

$$\frac{v_i}{v_o} = \frac{-([I]-[E]+appK_i) + \sqrt{([I]-[E]+appK_i)^2 + 4[E]*appK_i}}{2[E]} \quad (1)$$

$$IC_{50} = K_i*(1+(S/K_m)) \quad (2)$$

Figure S1. Compound 6 demonstrates characteristics of a tight binding ATP competitive inhibitor of human RIP1 with a K_i of 1.5 nM. The correlation between IC_{50} and ATP concentrations fits a mutually competitive model with IC_{50} values increasing linearly with increasing substrate concentrations. Due to the potency of the compound and limitations on ATP concentrations tolerated by the detection system, small changes in IC_{50} were expected. Data points are shown as the average of n=2 to n=4 determinations with error bars from the standard deviations. The fitted line is from eq 2 with $K_i = 1.5 \pm 0.5$ nM and $K_m = 140 \pm 54$ μ M. The K_i agrees well with the IC_{50} value reported in the main text.



5. Compound 6 binding kinetics

To determine the off rate constant for Compound 6, a fluorescence polarization (FP) competitive binding assay was used. This assay utilizes a reversible fluorescent ligand ((14-(2-([3-(2-[4-(cyanomethyl)phenyl]amino)-6-[(5-cyclopropyl-1H-pyrazol-3-yl)amino]-4-pyrimidinyl]amino)propyl]amino)-2-oxoethyl)-16,16,18,18-tetramethyl-6,7,7a,8a,9,10,16,18-octahydrobenzo[2'',3'']indolizino[8'',7'':5',6']pyrano[3',2':3,4]pyrido-[1,2-a]indol-5-ium-2-sulfonate) that is competitive with ATP. In a typical experiment, 3.5 μ L of titrated inhibitor in buffer (50 mM Hepes pH7.5, 10 mM NaCl, 50 mM MgCl₂, 0.5 mM DTT, and 0.02% CHAPS) and 3.5 μ L of ligand in buffer were added to a 384 black low volume Greiner plate. Then 3.5 μ L of enzyme was added to the plate to initiate the reaction and the plate was immediately monitored kinetically for 50 minutes using an Analyst GT plate reader (excitation 530 nm; emission 580 nm; 561 nm dichroic), with the shortest time interval possible between reads to maximize data density. The final concentrations of enzyme and fluorescent ligand were 10 nM and 5 nM, respectively. The FP data was converted to the concentration of enzyme-ligand complex (EL) formed (eq 3) and measuring controls for the polarization of free (P_f) and bound (P_b) ligand, where P = observed polarization and g = g factor [Jameson and Mocz, 2005]. The resulting individual binding curves

obtained at each inhibitor concentration were fitted globally using KinTek Explorer to a competitive model which describes both ligand binding and inhibitor binding equilibria ($E + L \rightleftharpoons EL$ and $E + I \rightleftharpoons EI$), where E = enzyme, L = ligand, EL = enzyme ligand complex, I = inhibitor, EI = enzyme inhibitor complex, k_1 = association rate of ligand, k_2 = dissociation rate of ligand, k_3 = association rate of inhibitor, and k_4 = dissociation rate of inhibitor. Multiple iterations of fitting were utilized until rates converged on a global minimum.

$$[EL] = L * \frac{(3-P_b)(P-P_f)}{(3-P)(P_b-P_f) + (g-1)(3-P_f)(P_b-P)} \quad (3)$$

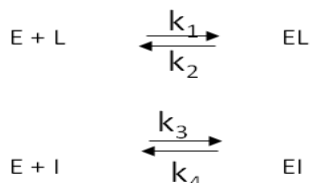
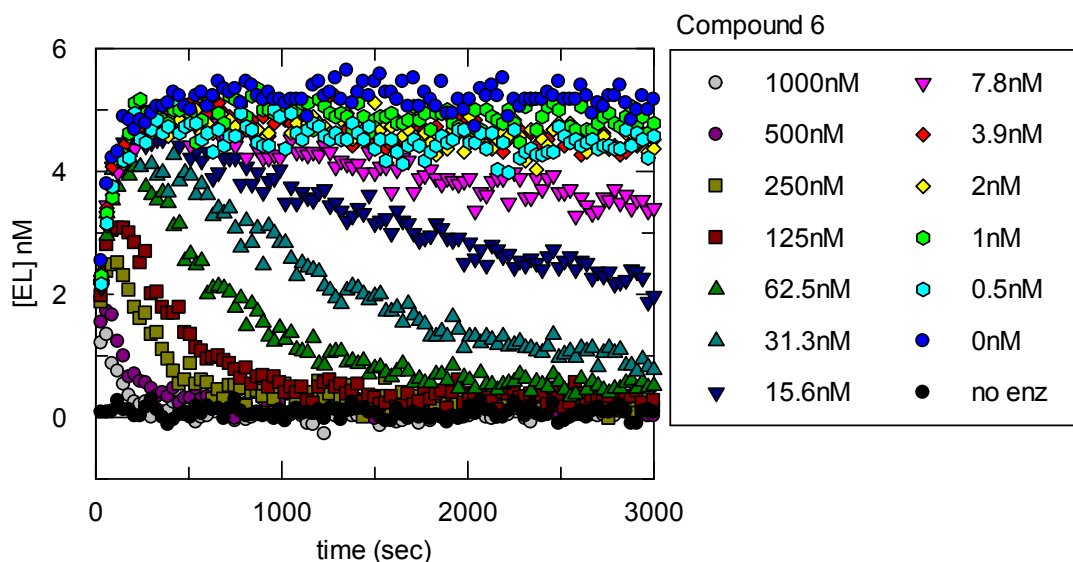


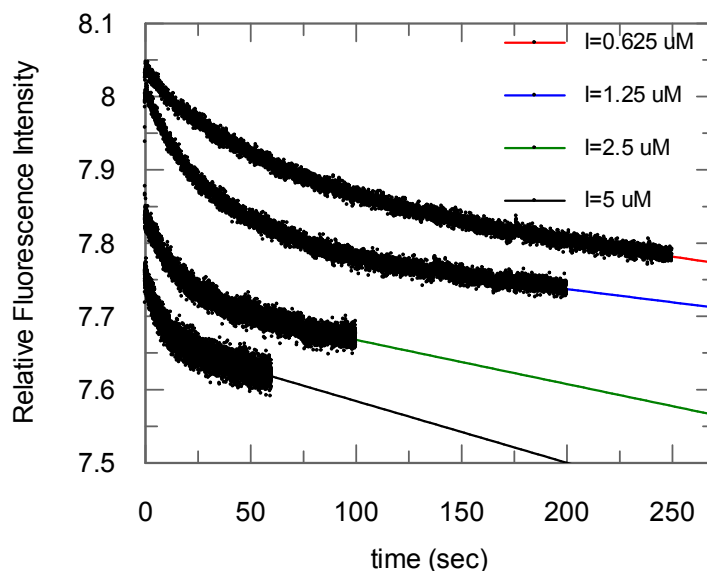
Figure S2. Compound 6 is a slowly dissociating inhibitor of hRIP1 ($k_{off} = 0.000117 \text{ sec}^{-1}$), demonstrating distinctive biphasic kinetics in an FP competitive binding assay. The other parameters from the average of $n=2$ global fits were $k_1 = 0.0526 \text{ nM}^{-1}\text{s}^{-1}$, $k_2 = 0.00265 \text{ s}^{-1}$, and $k_3 = 0.00210 \text{ nM}^{-1}\text{s}^{-1}$. k_3 for Compound 6 is poorly defined in this experiment due to insufficient data density for accurate measurement of rapid inhibitor association. Stopped-flow tryptophan fluorescence was used for accurate measurement of k_{on} as described below.

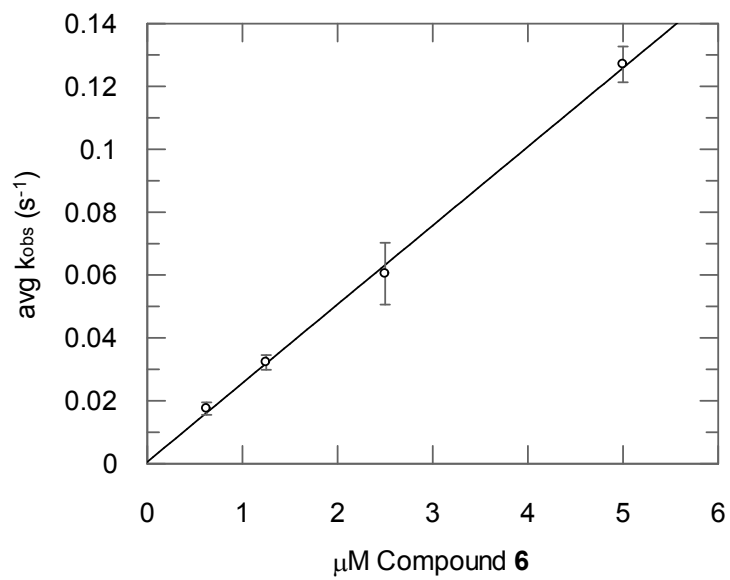


To determine the on rate constant of Compound 6 accurately, changes in the intrinsic tryptophan fluorescence of hRIP1 were measured upon inhibitor binding. Compound 6 was titrated (0.625 to 5 μM final) at 2x in buffer (50 mM Hepes pH 7.5, 10 mM NaCl, 50 mM MgCl_2 , 0.5 mM DTT, 0.02% CHAPS) with 1% DMSO. 250 nM (final) hRIP1 (1-375) was prepared in buffer at 2x. Inhibitor and enzyme were rapidly mixed using an Applied Photophysics SX20 stopped-flow spectrometer (fluorescence mode, 10 mm pathlength flow cell orientation, excitation 285 nm, emission $>320 \text{ nm}$, bandpass filter). PM voltage was set to approximately 80% of auto PM determined after mixing equal volumes of RIP1 and buffer. After determining this baseline, enzyme and inhibitor were rapidly mixed and 10,000 data time points were collected for up to 200 seconds for each inhibitor concentration, starting with the lowest inhibitor concentration.

Decreased fluorescence upon compound 6 binding was observed. Progress curves were averaged ($n=3$ to $n=4$) and fitted to a single exponential plus a slope to determine the k_{obs} at each inhibitor concentration. k_{obs} was then plotted as a function of inhibitor concentration and increased linearly with increasing inhibitor concentrations suggesting simple one-step binding mechanisms in the concentration range studied. The slope of the linear fit is equal to the on rate constant for Compound 6.

Figure S3. Compound 6 quenches intrinsic Trp fluorescence in the stopped-flow spectrometer consistent with a single step binding mechanism with an on rate constant of $0.025 \mu\text{M}^{-1}\text{s}^{-1}$. The top figure below shows representative stopped-flow time courses for different concentrations of compound 6 with hRIP1. Data were fitted to a single exponential decay with a linear slope (solid lines): $Y = A*(\exp(-k_{\text{obs}}*t) + b*t + C$. The slope portion of the fit is due to photobleaching of the enzyme and is also observed in control experiments in the absence of inhibitor. The average k_{obs} values and their standard errors from 3 to 4 determinations are replotted versus inhibitor concentration in the lower figure to obtain the on rate constant from the slope ($0.025 \pm 0.007 \mu\text{M}^{-1}\text{s}^{-1}$) of the linear fit (correlation coefficient = 0.9992). Intercepts of the replot (k_{off}) are poorly defined ($0.00053 \pm 0.0020 \text{ s}^{-1}$) due to extreme extrapolation from the K_i ($\sim 3,000 * K_i$ at $5 \mu\text{M}$). Therefore, k_{off} was measured using the FP competition assay (see above). The calculated K_i from the measured k_{off} and k_{on} values ($K_i = k_{\text{off}}/k_{\text{on}}$) is 4.7 nM , which is good agreement with the K_i from the ATP substrate competition experiment.





6. Compound 6 kinase selectivity and species selectivity profiles

Percent Enzyme Inhibition against Reaction Biology Corporation (RBC) kinase Panel

Compound 6 was tested at 10 μ M in duplicate against 359 kinases in the Reaction Biology Corporation (RBC) kinase panel. Control compound was tested in 10-dose IC₅₀ mode with 3-fold serial dilution starting at 20 μ M. Reactions were carried out at 10 μ M ATP. Full protocol details are available at <http://www.reactionbiology.com>. Data is reported as % enzyme activity (relative to DMSO controls) in Table S1. Activity <50% (average of n =2) was observed for ABL1, ABL2/ARG, BLK, c-Src, DDR2, EPHA5, EPHB2, FGR, FRK/PTK5, FYN, LYN, LYN B, PEAK1 and YES/YES1. However full curve analysis for these 14 kinases against compound 6 at a top concentration of 30 μ M (see Table S2) found no inhibition indicating the initial single concentration findings were false positives. The kinase panel did not include RIP1.

Table S1. RBC kinase panel for compound 6.

RBC Kinase:	Cpd 6 % enzyme activity	Cpd 6 % enzyme activity	Cpd 6 Average % enzyme activity	IC ₅₀ (M) Staurosporine	IC ₅₀ (M) Alternate Control cpd	Alternate compound ID
ABL1	6.77	6.20	6.49	5.20E-08		
ABL2/ARG	2.66	1.98	2.32	1.70E-08		
ACK1	91.64	90.81	91.23	3.44E-08		
AKT1	87.09	87.06	87.08	3.97E-09		
AKT2	80.42	78.39	79.40	1.40E-08		
AKT3	115.12	110.12	112.62	3.92E-09		
ALK	96.74	96.03	96.39	1.91E-09		
ALK1/ACVRL1	79.12	77.54	78.33	ND	7.30E-09	LDN193189
ALK2/ACVR1	101.76	97.57	99.67	ND	1.06E-07	LDN193189
ALK3/BMPR1A	95.61	95.25	95.43	ND	1.80E-08	LDN193189
ALK4/ACVR1B	104.11	102.81	103.46	ND	3.95E-07	LDN193189
ALK5/TGFBR1	97.00	96.12	96.56	ND	3.73E-07	LDN193189
ALK6/BMPR1B	97.00	96.84	96.92	ND	8.73E-09	LDN193189
ARAF	93.91	91.18	92.55	ND	1.74E-08	GW5074
ARK5/NUAK1	84.06	82.84	83.45	1.03E-09		
ASK1/MAP3K5	99.55	98.59	99.07	1.52E-08		
Aurora A	96.25	90.41	93.33	1.23E-09		
Aurora B	90.54	89.44	89.99	8.43E-09		
Aurora C	103.29	100.76	102.02	2.59E-09		
AXL	101.33	97.94	99.64	1.45E-08		
BLK	37.56	36.30	36.93	1.76E-09		
BMPR2	114.18	110.70	112.44	3.82E-07		
BMX/ETK	91.08	89.97	90.52	9.60E-09		
BRAF	96.93	96.90	96.91	ND	2.40E-08	GW5074
BRK	95.77	95.33	95.55	3.92E-07		
BRSK1	99.91	99.08	99.50	1.16E-09		
BRSK2	96.20	96.18	96.19	3.09E-09		
BTK	58.55	58.53	58.54	1.48E-08		
c-Kit	87.39	82.06	84.72	9.13E-08		
c-MER	94.84	93.66	94.25	1.03E-08		
c-MET	87.14	86.23	86.69	1.49E-07		
c-Src	2.15	1.91	2.03	2.71E-09		
CAMK1a	94.63	93.64	94.13	2.04E-09		

CAMK1b	93.25	88.96	91.10	4.36E-09		
CAMK1d	95.85	95.23	95.54	3.25E-10		
CAMK1g	96.61	95.87	96.24	8.92E-09		
CAMK2a	97.99	97.43	97.71	<7.63E-11		
CAMK2b	96.32	95.35	95.84	1.09E-10		
CAMK2d	103.56	102.81	103.18	<7.63E-11		
CAMK2g	97.11	95.46	96.29	4.50E-10		
CAMK4	95.72	94.55	95.14	2.17E-07		
CAMKK1	102.26	99.14	100.70	5.12E-08		
CAMKK2	87.11	87.10	87.10	7.94E-08		
CDC7/DBF4	105.23	104.87	105.05	1.75E-08		
CDK1/cyclin A	96.06	95.11	95.59	3.25E-09		
CDK1/cyclin B	93.94	92.83	93.38	2.40E-09		
CDK1/cyclin E	95.96	95.50	95.73	3.90E-09		
CDK16/cyclin Y (PCTAIRE)	96.33	95.36	95.85	1.21E-08		
CDK2/cyclin A	77.94	77.79	77.86	8.69E-10		
CDK2/Cyclin A1	90.13	89.11	89.62	2.03E-09		
CDK2/cyclin E	88.79	88.75	88.77	1.97E-09		
CDK3/cyclin E	87.06	86.34	86.70	1.56E-08		
CDK4/cyclin D1	97.97	97.88	97.92	1.92E-08		
CDK4/cyclin D3	91.73	89.31	90.52	3.46E-08		
CDK5/p25	72.38	70.42	71.40	3.32E-09		
CDK5/p35	71.11	70.78	70.95	1.87E-09		
CDK6/cyclin D1	96.81	95.26	96.04	5.51E-09		
CDK6/cyclin D3	99.65	99.02	99.33	6.39E-08		
CDK7/cyclin H	109.10	108.38	108.74	2.95E-06		
CDK9/cyclin K	99.55	97.49	98.52	1.51E-07		
CDK9/cyclin T1	98.66	98.54	98.60	1.32E-08		
CHK1	96.75	96.12	96.43	1.33E-10		
CHK2	102.74	101.65	102.19	8.90E-09		
CK1a1	92.67	92.43	92.55	4.05E-06		
CK1d	86.78	86.25	86.51	ND	1.81E-07	D4476
CK1epsilon	103.81	103.81	103.81	ND	2.51E-07	D4476
CK1g1	88.16	87.30	87.73	5.20E-06		
CK1g2	102.21	101.26	101.74	1.45E-06		
CK1g3	104.51	103.19	103.85	2.92E-06		
CK2a	120.74	118.67	119.71	ND	9.19E-08	GW5074
CK2a2	70.76	67.19	68.98	3.78E-07		
CLK1	97.07	96.74	96.90	1.42E-08		
CLK2	76.32	72.29	74.31	5.21E-09		
CLK3	97.80	97.10	97.45	2.24E-06		
CLK4	91.83	87.35	89.59	5.38E-08		
COT1/MAP3K8	98.66	97.48	98.07	ND	8.25E-06	Ro-31-8220
CSK	66.48	66.39	66.43	1.67E-08		
CTK/MATK	97.58	97.08	97.33	7.64E-07		
DAPK1	101.95	100.21	101.08	8.80E-09		
DAPK2	98.98	98.74	98.86	8.33E-09		
DCAMKL1	93.82	93.65	93.74	5.02E-07		
DCAMKL2	95.15	95.03	95.09	7.96E-08		
DDR1	97.18	96.12	96.65	4.66E-09		
DDR2	42.56	39.43	40.99	2.97E-10		
DLK/MAP3K12	86.36	85.32	85.84	1.08E-08		
DMPK	109.01	108.60	108.81	1.08E-07		
DMPK2	97.32	96.19	96.75	9.99E-10		
DRAK1/STK17A	94.60	94.47	94.53	1.52E-08		

DYRK1/DYRK1A	95.83	95.53	95.68	3.88E-09		
DYRK1B	94.25	92.81	93.53	9.89E-10		
DYRK2	113.90	102.05	107.98	2.29E-07		
DYRK3	104.84	103.52	104.18	3.22E-08		
DYRK4	94.55	93.07	93.81	ND	2.41E-06	GW5074
EGFR	103.89	101.58	102.74	1.31E-07		
EPHA1	95.74	95.49	95.62	1.59E-07		
EPHA2	88.30	85.42	86.86	4.94E-08		
EPHA3	96.98	95.60	96.29	4.47E-08		
EPHA4	78.45	77.84	78.15	1.94E-08		
EPHA5	34.25	34.19	34.22	2.14E-08		
EPHA6	93.79	92.47	93.13	1.80E-08		
EPHA7	102.02	99.67	100.85	4.22E-08		
EPHA8	97.87	94.67	96.27	1.21E-07		
EPHB1	57.22	57.17	57.20	3.67E-08		
EPHB2	29.79	29.04	29.42	1.13E-07		
EPHB3	84.00	82.17	83.09	1.26E-06		
EPHB4	83.35	82.60	82.98	2.15E-07		
ERBB2/HER2	96.84	96.54	96.69	1.67E-07		
ERBB4/HER4	94.38	93.16	93.77	2.48E-07		
ERK1	98.69	98.08	98.39	2.22E-05		
ERK2/MAPK1	93.84	92.41	93.12	1.40E-05		
ERK5/MAPK7	98.97	97.08	98.02	1.64E-05		
ERK7/MAPK15	102.85	97.48	100.16	1.04E-08		
FAK/PTK2	91.46	91.22	91.34	1.42E-08		
FER	87.13	84.85	85.99	3.83E-10		
FES/FPS	93.66	92.20	92.93	2.57E-09		
FGFR1	97.67	95.89	96.78	7.63E-09		
FGFR2	95.53	93.73	94.63	2.40E-09		
FGFR3	100.72	97.77	99.24	1.94E-08		
FGFR4	90.19	89.43	89.81	1.88E-07		
FGR	6.11	5.54	5.83	1.07E-09		
FLT1/VEGFR1	96.55	95.29	95.92	9.77E-09		
FLT3	92.34	91.87	92.10	1.75E-09		
FLT4/VEGFR3	94.76	93.61	94.19	3.34E-09		
FMS	96.86	95.35	96.10	2.76E-09		
FRK/PTK5	46.41	46.19	46.30	1.90E-08		
FYN	5.09	4.18	4.63	1.64E-09		
GCK/MAP4K2	96.08	95.50	95.79	5.30E-10		
GLK/MAP4K3	93.85	92.56	93.20	1.68E-10		
GRK1	105.64	105.37	105.50	6.88E-08		
GRK2	101.50	100.40	100.95	1.41E-06		
GRK3	98.05	97.68	97.86	9.75E-07		
GRK4	100.83	98.85	99.84	9.74E-08		
GRK5	104.05	103.32	103.69	8.90E-08		
GRK6	97.75	91.33	94.54	4.32E-08		
GRK7	101.47	99.04	100.26	5.51E-09		
GSK3a	99.34	97.33	98.33	6.54E-09		
GSK3b	102.29	100.84	101.57	5.14E-09		
Haspin	98.69	95.61	97.15	2.58E-08		
HCK	84.35	83.94	84.15	2.06E-09		
HGK/MAP4K4	93.86	92.82	93.34	5.58E-10		
HIPK1	110.64	107.89	109.27	ND	2.36E-07	Ro-31-8220
HIPK2	96.52	95.26	95.89	5.95E-07		
HIPK3	102.38	102.11	102.25	1.08E-06		

HIPK4	98.85	98.04	98.45	3.93E-07		
HPK1/MAP4K1	94.41	94.05	94.23	ND	2.42E-08	Ro-31-8220
IGF1R	96.54	96.38	96.46	5.76E-08		
IKKa/CHUK	109.12	107.50	108.31	1.30E-07		
IKKb/IKBKB	106.03	103.84	104.93	5.45E-07		
IKKe/IKBKE	99.79	99.08	99.43	3.50E-10		
IR	91.43	90.38	90.91	1.60E-08		
IRAK1	114.99	114.14	114.57	5.41E-08		
IRAK4	94.01	92.76	93.39	3.84E-09		
IRR/INSRR	94.69	94.54	94.62	1.64E-08		
ITK	101.59	101.46	101.53	1.29E-08		
JAK1	87.31	86.98	87.15	3.89E-10		
JAK2	74.70	73.98	74.34	3.94E-10		
JAK3	107.13	103.55	105.34	1.04E-10		
JNK1	98.67	95.39	97.03	8.29E-07		
JNK2	102.91	101.90	102.40	2.53E-06		
JNK3	97.84	97.07	97.45	ND	3.06E-07	JNKi VIII
KDR/VEGFR2	96.26	95.64	95.95	1.12E-08		
KHS/MAP4K5	93.05	92.03	92.54	2.41E-10		
LATS1	99.84	98.07	98.96	9.89E-09		
LATS2	93.09	91.19	92.14	5.78E-09		
LCK	72.09	71.93	72.01	1.76E-09		
LCK2/ICK	92.03	89.55	90.79	4.29E-08		
LIMK1	92.18	89.27	90.73	2.91E-09		
LIMK2	73.30	71.69	72.50	1.30E-07		
LKB1	96.36	96.34	96.35	8.20E-08		
LOK/STK10	93.17	91.56	92.36	1.19E-08		
LRRK2	92.09	90.68	91.38	9.37E-09		
LYN	6.05	5.84	5.95	8.68E-10		
LYN B	4.87	3.79	4.33	4.34E-09		
MAPKAPK2	96.32	94.01	95.16	1.35E-07		
MAPKAPK3	102.78	102.56	102.67	5.27E-06		
MAPKAPK5/PRAK	96.99	96.47	96.73	3.41E-07		
MARK1	91.66	89.71	90.68	2.15E-10		
MARK2/PAR-1Ba	95.01	94.69	94.85	1.13E-10		
MARK3	103.83	101.56	102.69	2.93E-10		
MARK4	100.61	98.61	99.61	1.21E-10		
MEK1	108.30	103.84	106.07	3.12E-08		
MEK2	99.21	96.54	97.88	4.35E-08		
MEK3	99.86	99.42	99.64	2.32E-08		
MEKK1	102.71	101.55	102.13	5.69E-07		
MEKK2	87.97	86.69	87.33	1.33E-08		
MEKK3	115.34	112.06	113.70	4.63E-08		
MELK	109.87	106.01	107.94	6.89E-10		
MINK/MINK1	100.20	100.15	100.18	7.34E-10		
MKK4	100.45	98.92	99.69	1.64E-06		
MKK6	104.87	103.90	104.38	5.99E-09		
MLCK/MYLK	97.72	96.93	97.32	8.77E-08		
MLCK2/MYLK2	98.81	97.10	97.95	1.61E-08		
MLK1/MAP3K9	98.49	98.16	98.33	1.55E-09		
MLK2/MAP3K10	98.73	97.91	98.32	2.69E-09		
MLK3/MAP3K11	96.99	96.30	96.64	3.65E-09		
MNK1	98.24	95.68	96.96	5.58E-08		
MNK2	100.00	99.65	99.83	2.04E-08		
MRCKa/CDC42BPA	98.42	98.09	98.26	6.71E-09		

MRCKb/CDC42BPB	92.25	90.15	91.20	3.59E-09		
MSK1/RPS6KA5	108.19	102.06	105.13	6.90E-10		
MSK2/RPS6KA4	85.22	80.69	82.96	1.83E-09		
MSSK1/STK23	94.21	93.52	93.86	1.62E-06		
MST1/STK4	92.18	91.01	91.60	1.78E-09		
MST2/STK3	101.32	101.13	101.23	3.32E-09		
MST3/STK24	98.06	96.35	97.21	2.62E-09		
MST4	97.08	96.58	96.83	3.34E-09		
MUSK	90.73	84.02	87.38	1.21E-07		
MYLK3	99.90	98.98	99.44	1.82E-07		
MYO3b	98.51	98.32	98.42	5.17E-09		
NEK1	94.87	94.75	94.81	1.73E-08		
NEK11	104.83	103.72	104.28	1.31E-06		
NEK2	98.70	98.07	98.38	5.07E-07		
NEK3	106.32	106.18	106.25	>2.00E-05		
NEK4	104.65	101.59	103.12	6.81E-08		
NEK5	91.76	91.50	91.63	5.93E-08		
NEK6	93.92	91.10	92.51	ND	8.34E-06	PKR Inhibitor
NEK7	94.45	91.32	92.88	ND	2.19E-06	PKR Inhibitor
NEK9	96.89	96.87	96.88	1.04E-07		
NLK	96.33	95.12	95.73	5.84E-08		
OSR1/OXSR1	98.34	97.62	97.98	6.87E-08		
P38a/MAPK14	104.67	100.89	102.78	ND	2.04E-08	SB202190
P38b/MAPK11	99.09	96.41	97.75	ND	2.64E-08	SB202190
P38d/MAPK13	97.05	95.83	96.44	1.21E-07		
P38g	99.70	98.20	98.95	2.18E-07		
p70S6K/RPS6KB1	99.96	98.35	99.16	5.69E-10		
p70S6Kb/RPS6KB2	99.73	94.93	97.33	2.67E-09		
PAK1	100.66	100.28	100.47	5.07E-10		
PAK2	99.49	99.36	99.43	2.96E-09		
PAK3	102.06	99.32	100.69	4.12E-10		
PAK4	94.18	93.46	93.82	2.26E-08		
PAK5	102.54	102.43	102.48	3.25E-09		
PAK6	99.31	98.98	99.15	6.22E-08		
PASK	94.22	91.31	92.77	1.56E-08		
PBK/TOPK	109.73	105.61	107.67	9.35E-08		
PDGFRa	80.16	78.21	79.19	8.16E-10		
PDGFRb	90.17	89.87	90.02	3.17E-09		
PDK1/PDPK1	105.07	104.15	104.61	4.64E-10		
PHKg1	100.03	99.30	99.67	2.53E-09		
PHKg2	95.49	94.40	94.95	1.03E-09		
PIM1	98.98	98.46	98.72	5.11E-09		
PIM2	103.09	100.81	101.95	4.07E-08		
PIM3	94.43	94.10	94.27	1.34E-10		
PKA	95.32	92.90	94.11	9.30E-10		
PKAcb	107.21	105.48	106.35	1.52E-09		
PKAcb	105.86	103.91	104.89	5.93E-09		
PKCa	98.43	97.92	98.18	3.55E-10		
PKCb1	100.11	98.20	99.16	1.44E-08		
PKCb2	90.98	90.22	90.60	1.93E-09		
PKCd	120.04	104.26	112.15	1.83E-10		
PKCepsilon	96.07	96.02	96.05	2.23E-10		
PKCeta	93.92	93.02	93.47	1.06E-09		
PKCg	94.74	92.05	93.40	1.38E-09		
PKCiota	106.04	102.11	104.07	2.31E-08		

PKCmu/PRKD1	92.08	91.08	91.58	1.48E-09		
PKCnu/PRKD3	96.95	95.64	96.30	9.09E-10		
PKCtheta	119.64	118.21	118.92	9.29E-10		
PKCzeta	102.04	99.30	100.67	7.08E-08		
PKD2/PRKD2	92.68	91.17	91.92	1.39E-09		
PKG1a	97.71	96.74	97.23	3.69E-09		
PKG1b	82.34	80.94	81.64	3.64E-09		
PKG2/PRKG2	85.23	83.94	84.59	1.48E-08		
PKN1/PRK1	120.19	112.74	116.46	4.98E-09		
PKN2/PRK2	112.91	103.99	108.45	3.31E-09		
PKN3/PRK3	104.94	103.91	104.43	1.09E-08		
PLK1	104.21	103.78	103.99	2.53E-07		
PLK2	97.07	96.93	97.00	2.53E-07		
PLK3	106.53	106.30	106.42	2.01E-07		
PLK4/SAK	96.09	94.23	95.16	8.67E-09		
PRKX	111.62	110.34	110.98	2.48E-09		
PYK2	96.91	96.69	96.80	9.12E-09		
RAF1	95.81	95.72	95.76	ND	1.05E-08	GW5074
RET	94.38	92.20	93.29	2.32E-09		
RIPK2	82.99	82.97	82.98	4.35E-07		
RIPK3	96.14	95.74	95.94	ND	2.31E-06	GW5074
RIPK5	89.60	86.62	88.11	4.98E-08		
ROCK1	106.95	104.53	105.74	7.65E-10		
ROCK2	99.31	98.41	98.86	6.52E-10		
RON/MST1R	97.13	95.42	96.28	2.10E-07		
ROS/ROS1	93.73	93.10	93.42	1.74E-10		
RSK1	101.49	99.55	100.52	1.72E-10		
RSK2	94.19	91.17	92.68	1.23E-10		
RSK3	100.51	99.79	100.15	2.69E-10		
RSK4	87.08	86.68	86.88	1.29E-10		
SGK1	81.36	81.15	81.26	8.66E-09		
SGK2	97.02	96.25	96.64	1.27E-08		
SGK3/SGKL	102.96	102.15	102.55	1.76E-07		
SIK1	72.05	71.52	71.78	6.22E-10		
SIK2	67.31	66.61	66.96	3.14E-10		
SIK3	90.94	89.92	90.43	5.21E-10		
SLK/STK2	105.12	100.76	102.94	1.70E-08		
SNARK/NUAK2	105.01	104.88	104.95	3.12E-08		
SRMS	93.70	93.47	93.58	8.92E-06		
SRPK1	93.37	89.31	91.34	2.85E-08		
SRPK2	108.84	106.63	107.73	2.80E-07		
SSTK/TSSK6	100.55	100.43	100.49	1.46E-07		
STK16	100.64	99.37	100.01	2.47E-07		
STK22D/TSSK1	85.75	83.51	84.63	<7.63E-11		
STK25/YSK1	105.35	103.12	104.24	2.00E-09		
STK32B/YANK2	104.24	99.86	102.05	1.57E-07		
STK32C/YANK3	101.00	99.55	100.27	3.83E-07		
STK33	81.99	80.40	81.20	3.78E-08		
STK38/NDR1	93.73	90.14	91.94	1.15E-08		
STK38L/NDR2	94.69	94.19	94.44	1.28E-09		
STK39/STLK3	94.61	93.13	93.87	2.62E-08		
SYK	98.07	97.76	97.91	4.63E-10		
TAK1	101.50	101.43	101.47	5.07E-08		
TAOK1	97.98	95.83	96.91	1.22E-09		
TAOK2/TAO1	100.70	100.63	100.66	7.44E-09		

TAOK3/JIK	93.92	92.17	93.05	2.02E-09		
TBK1	99.74	96.45	98.09	3.03E-09		
TEC	98.65	97.03	97.84	5.74E-08		
TESK1	102.49	100.97	101.73	6.26E-07		
TGFBR2	102.81	100.94	101.87	ND	8.99E-08	LDN193189
TIE2/TEK	98.54	97.93	98.23	8.30E-08		
TLK1	106.35	104.34	105.34	2.16E-08		
TLK2	103.67	102.60	103.13	3.10E-09		
TNIK	94.42	93.91	94.17	4.84E-10		
TNK1	94.72	93.86	94.29	2.26E-09		
TRKA	91.21	89.91	90.56	1.53E-09		
TRKB	97.13	96.67	96.90	9.34E-11		
TRKC	84.82	84.44	84.63	2.84E-10		
TSSK2	100.89	100.69	100.79	6.02E-09		
TSSK3/STK22C	109.54	107.61	108.58	5.33E-09		
TTBK1	100.31	99.10	99.71	ND	>2.00E-05	SB202190
TTBK2	121.19	116.68	118.93	ND	7.51E-06	SB202190
TXK	86.65	84.62	85.63	3.60E-08		
TYK1/LTK	98.59	97.10	97.84	2.97E-08		
TYK2	95.80	95.18	95.49	2.44E-10		
TYRO3/SKY	98.80	98.45	98.62	3.55E-09		
ULK1	98.97	97.19	98.08	7.58E-09		
ULK2	104.09	98.50	101.29	2.01E-09		
ULK3	93.04	91.84	92.44	6.61E-09		
VRK1	120.44	115.26	117.85	ND	9.85E-07	Ro-31-8220
VRK2	86.70	82.46	84.58	ND	2.80E-05	Ro-31-8220
WEE1	109.20	105.61	107.41	ND	6.66E-07	Wee-1 Inhibitor
WNK1	91.91	94.67	93.29	1.26E-05		
WNK2	96.75	94.80	95.78	1.15E-06		
WNK3	97.09	95.89	96.49	ND	2.51E-06	Wee-1 Inhibitor
YES/YES1	34.10	32.74	33.42	2.78E-09		
ZAK/MLTK	100.02	96.37	98.20	ND	1.32E-06	GW5074
ZAP70	102.08	101.00	101.54	1.05E-08		
ZIPK/DAPK3	106.51	105.14	105.82	2.69E-09		
CDK14/cyclin Y (PFTK1)	98.67	98.02	98.35	4.76E-08		
CDK17/cyclin Y (PCTK2)	92.57	92.40	92.49	1.19E-08		
CDK18/cyclin Y (PCTK3)	101.88	99.59	100.73	2.20E-08		
CDK2/cyclin O	83.78	81.25	82.51	1.67E-09		
CK1a1L	99.76	94.67	97.22	1.85E-06		
ERN2/IRE2	89.64	89.47	89.55	3.68E-08		
KSR1	102.47	102.08	102.28	7.88E-06		
KSR2	103.24	101.04	102.14	4.44E-06		
MAK	98.27	97.98	98.12	2.40E-08		
MEKK6	96.98	96.26	96.62	6.06E-07		
MKK7	98.63	97.72	98.17	6.13E-07		
MLK4	97.17	94.42	95.80	6.94E-07		
MYO3A	99.87	96.96	98.41	2.11E-08		
NIM1	103.86	103.47	103.67	1.38E-07		
PEAK1	0.03	-0.19	-0.08	2.87E-09		
STK21/CIT	100.89	100.35	100.62	5.81E-07		
YSK4/MAP3K19	104.33	103.40	103.86	1.78E-08		

Table S2. Selected RBC kinase IC₅₀'s for compound **6**.

ABL			
Cpd 6 conc.(M)	Enzyme activity	Staurosporine Conc.(M)	Enzyme activity
3.00E-05	98.33	2.00E-05	2.74
1.00E-05	92.94	5.00E-06	7.07
3.33E-06	97.16	1.25E-06	7.05
1.11E-06	94.95	3.13E-07	19.95
3.70E-07	107.79	7.81E-08	50.45
1.23E-07	96.59	1.95E-08	81.15
4.12E-08	97.49	4.88E-09	89.98
1.37E-08	93.19	1.22E-09	93.89
4.57E-09	90.31	3.05E-10	97.84
1.52E-09	97.70	7.63E-11	97.27
DMSO	97.58	DMSO	102.42
ABL2/ARG			
Cpd 6 conc.(M)	Enzyme activity	Staurosporine Conc.(M)	Enzyme activity
3.00E-05	104.12	2.00E-05	0.61
1.00E-05	100.40	5.00E-06	4.26
3.33E-06	102.36	1.25E-06	-1.38
1.11E-06	95.38	3.13E-07	7.51
3.70E-07	107.27	7.81E-08	24.18
1.23E-07	100.95	1.95E-08	56.54
4.12E-08	93.52	4.88E-09	81.06
1.37E-08	103.77	1.22E-09	95.09
4.57E-09	99.09	3.05E-10	101.43
1.52E-09	104.61	7.63E-11	105.90
DMSO	102.74	DMSO	97.26
BLK			
Cpd 6 conc.(M)	Enzyme activity	Staurosporine Conc.(M)	Enzyme activity
3.00E-05	105.18	2.00E-05	0.80
1.00E-05	114.05	5.00E-06	0.08
3.33E-06	115.89	1.25E-06	0.00
1.11E-06	109.10	3.13E-07	1.44
3.70E-07	111.82	7.81E-08	0.75
1.23E-07	104.12	1.95E-08	7.82
4.12E-08	92.30	4.88E-09	22.55
1.37E-08	104.06	1.22E-09	53.54
4.57E-09	107.30	3.05E-10	85.52
1.52E-09	102.44	7.63E-11	98.94
DMSO	102.34	DMSO	97.66
c-Src			
Cpd 6 conc.(M)	Enzyme activity	Staurosporine Conc.(M)	Enzyme activity
3.00E-05	104.49	2.00E-05	0.45

1.00E-05	105.26	5.00E-06	0.20
3.33E-06	106.77	1.25E-06	0.93
1.11E-06	106.08	3.13E-07	0.59
3.70E-07	110.78	7.81E-08	4.41
1.23E-07	103.01	1.95E-08	15.49
4.12E-08	102.80	4.88E-09	43.50
1.37E-08	107.86	1.22E-09	76.88
4.57E-09	105.08	3.05E-10	95.14
1.52E-09	102.59	7.63E-11	101.02
DMSO	100.72	DMSO	99.28
DDR2			
Cpd 6 conc.(M)	Enzyme activity	Staurosporine Conc.(M)	Enzyme activity
3.00E-05	96.47	2.00E-05	5.82
1.00E-05	112.30	5.00E-06	5.55
3.33E-06	103.48	1.25E-06	6.04
1.11E-06	100.72	3.13E-07	2.66
3.70E-07	107.16	7.81E-08	7.44
1.23E-07	106.72	1.95E-08	0.98
4.12E-08	99.08	4.88E-09	6.55
1.37E-08	100.39	1.22E-09	8.95
4.57E-09	102.20	3.05E-10	27.48
1.52E-09	94.46	7.63E-11	66.47
DMSO	100.33	DMSO	99.67
EPHA5			
Cpd 6 conc.(M)	Enzyme activity	Staurosporine Conc.(M)	Enzyme activity
3.00E-05	100.32	2.00E-05	3.30
1.00E-05	98.01	5.00E-06	0.12
3.33E-06	100.04	1.25E-06	3.46
1.11E-06	101.68	3.13E-07	13.03
3.70E-07	104.14	7.81E-08	33.81
1.23E-07	98.64	1.95E-08	63.75
4.12E-08	103.74	4.88E-09	85.84
1.37E-08	101.31	1.22E-09	98.24
4.57E-09	96.20	3.05E-10	97.83
1.52E-09	96.21	7.63E-11	99.51
DMSO	97.41	DMSO	102.59
EPHB2			
Cpd 6 conc.(M)	Enzyme activity	Staurosporine Conc.(M)	Enzyme activity
3.00E-05	98.88	2.00E-05	2.53
1.00E-05	97.76	5.00E-06	4.92
3.33E-06	99.37	1.25E-06	15.99
1.11E-06	95.58	3.13E-07	40.87

3.70E-07	105.13	7.81E-08	79.40
1.23E-07	98.81	1.95E-08	94.41
4.12E-08	100.11	4.88E-09	96.73
1.37E-08	99.74	1.22E-09	98.77
4.57E-09	102.04	3.05E-10	102.23
1.52E-09	98.77	7.63E-11	104.62
DMSO	96.32	DMSO	103.68
FGR			
Cpd 6 conc.(M)	Enzyme activity	Staurosporine Conc.(M)	Enzyme activity
3.00E-05	96.37	2.00E-05	0.91
1.00E-05	100.80	5.00E-06	2.33
3.33E-06	97.69	1.25E-06	0.81
1.11E-06	97.44	3.13E-07	2.49
3.70E-07	102.69	7.81E-08	2.96
1.23E-07	100.61	1.95E-08	9.31
4.12E-08	98.83	4.88E-09	26.92
1.37E-08	101.46	1.22E-09	60.64
4.57E-09	102.36	3.05E-10	85.70
1.52E-09	94.16	7.63E-11	100.29
DMSO	100.08	DMSO	99.92
FRK/PTK5			
Cpd 6 conc.(M)	Enzyme activity	Staurosporine Conc.(M)	Enzyme activity
3.00E-05	96.26	2.00E-05	2.80
1.00E-05	99.42	5.00E-06	2.66
3.33E-06	99.23	1.25E-06	6.60
1.11E-06	100.58	3.13E-07	15.18
3.70E-07	105.20	7.81E-08	40.82
1.23E-07	101.95	1.95E-08	73.53
4.12E-08	97.18	4.88E-09	90.91
1.37E-08	99.10	1.22E-09	99.50
4.57E-09	102.00	3.05E-10	97.41
1.52E-09	97.05	7.63E-11	99.46
DMSO	101.41	DMSO	98.59
FYN			
Cpd 6 conc.(M)	Enzyme activity	Staurosporine Conc.(M)	Enzyme activity
3.00E-05	104.38	2.00E-05	1.53
1.00E-05	105.58	5.00E-06	1.32
3.33E-06	103.91	1.25E-06	-0.20
1.11E-06	106.37	3.13E-07	3.03
3.70E-07	110.39	7.81E-08	4.85
1.23E-07	105.07	1.95E-08	14.02
4.12E-08	107.06	4.88E-09	36.10

1.37E-08	102.69	1.22E-09	67.94
4.57E-09	105.18	3.05E-10	94.32
1.52E-09	105.12	7.63E-11	103.12
DMSO	101.35	DMSO	98.65
LYN			
Cpd 6 conc.(M)	Enzyme activity	Staurosporine Conc.(M)	Enzyme activity
3.00E-05	99.76	2.00E-05	-0.25
1.00E-05	105.03	5.00E-06	0.46
3.33E-06	103.88	1.25E-06	0.07
1.11E-06	104.13	3.13E-07	0.71
3.70E-07	108.88	7.81E-08	2.43
1.23E-07	105.71	1.95E-08	6.77
4.12E-08	111.22	4.88E-09	16.61
1.37E-08	109.72	1.22E-09	45.84
4.57E-09	107.08	3.05E-10	78.56
1.52E-09	101.33	7.63E-11	97.56
DMSO	98.94	DMSO	101.06
LYN B			
Cpd 6 conc.(M)	Enzyme activity	Staurosporine Conc.(M)	Enzyme activity
3.00E-05	104.27	2.00E-05	1.14
1.00E-05	99.43	5.00E-06	-1.81
3.33E-06	103.19	1.25E-06	0.78
1.11E-06	103.57	3.13E-07	5.95
3.70E-07	104.45	7.81E-08	12.51
1.23E-07	108.95	1.95E-08	27.74
4.12E-08	108.18	4.88E-09	58.22
1.37E-08	104.23	1.22E-09	95.35
4.57E-09	106.29	3.05E-10	98.96
1.52E-09	103.48	7.63E-11	100.07
DMSO	99.73	DMSO	100.27
PEAK1			
Cpd 6 conc.(M)	Enzyme activity	Staurosporine Conc.(M)	Enzyme activity
3.00E-05	97.38	2.00E-05	-0.03
1.00E-05	99.90	5.00E-06	0.20
3.33E-06	99.50	1.25E-06	2.21
1.11E-06	99.77	3.13E-07	0.96
3.70E-07	109.05	7.81E-08	5.86
1.23E-07	104.60	1.95E-08	13.85
4.12E-08	102.15	4.88E-09	39.71
1.37E-08	100.23	1.22E-09	73.35
4.57E-09	104.45	3.05E-10	91.74
1.52E-09	100.00	7.63E-11	94.28

DMSO	97.95	DMSO	102.05
YES/YES1			
Cpd 6 conc.(M)	Enzyme activity	Staurosporine Conc.(M)	Enzyme activity
3.00E-05	98.37	2.00E-05	0.44
1.00E-05	101.54	5.00E-06	0.36
3.33E-06	92.69	1.25E-06	1.15
1.11E-06	95.73	3.13E-07	1.44
3.70E-07	97.90	7.81E-08	4.49
1.23E-07	98.77	1.95E-08	13.93
4.12E-08	96.71	4.88E-09	35.62
1.37E-08	99.98	1.22E-09	68.42
4.57E-09	99.46	3.05E-10	90.41
1.52E-09	99.86	7.63E-11	95.15
DMSO	99.71	DMSO	100.29

Percent enzyme inhibition against DiscoverX KINOMEScan™ profiling service

Compound **6** was tested at 10 μ M in duplicate against 456 kinases (395 non-mutant kinases) in the DiscoverX KINOMEScan® kinase profile panel [Fabian, 2005] as shown in Table S3. ATP was not used in the KINOMEScan® competition binding assay platform (<http://www.discoverx.com>).

Table S3. DiscoverX kinase panel for compound **6**.

Kinase	% Enzyme Activity	Molar Conc (μ M)
ABL1(E255K)-phosphorylated	87	10000
ABL1(F317I)-nonphosphorylated	90	10000
ABL1(F317I)-phosphorylated	82	10000
ABL1(F317L)-nonphosphorylated	87	10000
ABL1(F317L)-phosphorylated	85	10000
ABL1(H396P)-nonphosphorylated	97	10000
ABL1(H396P)-phosphorylated	90	10000
ABL1(M351T)-phosphorylated	90	10000
ABL1(Q252H)-nonphosphorylated	96	10000
ABL1(Q252H)-phosphorylated	89	10000
ABL1(T315I)-nonphosphorylated	91	10000
ABL1(T315I)-phosphorylated	72	10000
ABL1(Y253F)-phosphorylated	77	10000
ABL1-nonphosphorylated	91	10000
ABL1-phosphorylated	78	10000
ABL2	94	10000
ACVR1	90	10000
ACVR1B	97	10000
ACVR2A	94	10000

ACVR2B	92	10000
ACVRL1	99	10000
ADCK3	100	10000
ADCK4	100	10000
AKT1	82	10000
AKT2	89	10000
AKT3	89	10000
ALK	100	10000
ALK(C1156Y)	84	10000
ALK(L1196M)	96	10000
AMPK-alpha1	86	10000
AMPK-alpha2	93	10000
ANKK1	88	10000
ARK5	100	10000
ASK1	100	10000
ASK2	77	10000
AURKA	84	10000
AURKB	89	10000
AURKC	82	10000
AXL	92	10000
BIKE	94	10000
BLK	93	10000
BMPR1A	84	10000
BMPR1B	81	10000
BMPR2	83	10000
BMX	95	10000
BRAF	87	10000
BRAF(V600E)	93	10000
BRK	100	10000
BRSK1	100	10000
BRSK2	100	10000
BTK	100	10000
BUB1	100	10000
CAMK1	52	10000
CAMK1D	58	10000
CAMK1G	97	10000
CAMK2A	100	10000
CAMK2B	100	10000
CAMK2D	97	10000
CAMK2G	90	10000
CAMK4	79	10000
CAMKK1	95	10000

CAMKK2	95	10000
CASK	87	10000
CDC2L1	100	10000
CDC2L2	94	10000
CDC2L5	63	10000
CDK11	83	10000
CDK2	98	10000
CDK3	100	10000
CDK4-cyclinD1	100	10000
CDK4-cyclinD3	81	10000
CDK5	91	10000
CDK7	79	10000
CDK8	100	10000
CDK9	96	10000
CDKL1	97	10000
CDKL2	100	10000
CDKL3	82	10000
CDKL5	83	10000
CHEK1	99	10000
CHEK2	98	10000
CIT	96	10000
CLK1	80	10000
CLK2	100	10000
CLK3	88	10000
CLK4	93	10000
CSF1R	83	10000
CSF1R-autoinhibited	94	10000
CSK	98	10000
CSNK1A1	82	10000
CSNK1A1L	87	10000
CSNK1D	88	10000
CSNK1E	86	10000
CSNK1G1	88	10000
CSNK1G2	94	10000
CSNK1G3	97	10000
CSNK2A1	96	10000
CSNK2A2	85	10000
CTK	88	10000
DAPK1	76	10000
DAPK2	81	10000
DAPK3	83	10000
DCAMKL1	69	10000

DCAMKL2	92	10000
DCAMKL3	92	10000
DDR1	99	10000
DDR2	100	10000
DLK	100	10000
DMPK	88	10000
DMPK2	90	10000
DRAK1	94	10000
DRAK2	91	10000
DYRK1A	84	10000
DYRK1B	86	10000
DYRK2	90	10000
EGFR	91	10000
EGFR(E746-A750del)	94	10000
EGFR(G719C)	97	10000
EGFR(G719S)	97	10000
EGFR(L747-E749del, A750P)	91	10000
EGFR(L747-S752del, P753S)	100	10000
EGFR(L747-T751del,Sins)	89	10000
EGFR(L858R)	93	10000
EGFR(L858R,T790M)	90	10000
EGFR(L861Q)	80	10000
EGFR(S752-I759del)	98	10000
EGFR(T790M)	92	10000
EIF2AK1	89	10000
EPHA1	100	10000
EPHA2	94	10000
EPHA3	94	10000
EPHA4	82	10000
EPHA5	93	10000
EPHA6	81	10000
EPHA7	94	10000
EPHA8	96	10000
EPHB1	92	10000
EPHB2	97	10000
EPHB3	91	10000
EPHB4	93	10000
EPHB6	100	10000
ERBB2	100	10000
ERBB3	100	10000
ERBB4	100	10000
ERK1	97	10000

ERK2	98	10000
ERK3	90	10000
ERK4	93	10000
ERK5	95	10000
ERK8	86	10000
ERN1	79	10000
FAK	96	10000
FER	87	10000
FES	87	10000
FGFR1	96	10000
FGFR2	100	10000
FGFR3	84	10000
FGFR3(G697C)	87	10000
FGFR4	100	10000
FGR	88	10000
FLT1	88	10000
FLT3	93	10000
FLT3(D835H)	99	10000
FLT3(D835Y)	89	10000
FLT3(ITD)	100	10000
FLT3(K663Q)	100	10000
FLT3(N841I)	95	10000
FLT3(R834Q)	100	10000
FLT3-autoinhibited	94	10000
FLT4	94	10000
FRK	100	10000
FYN	100	10000
GAK	100	10000
GCN2(Kin.Dom.2,S808G)	100	10000
GRK1	94	10000
GRK4	100	10000
GRK7	100	10000
GSK3A	96	10000
GSK3B	80	10000
HASPIN	78	10000
HCK	91	10000
HIPK1	75	10000
HIPK2	88	10000
HIPK3	86	10000
HIPK4	93	10000
HPK1	98	10000
HUNK	97	10000

ICK	81	10000
IGF1R	99	10000
IKK-alpha	99	10000
IKK-beta	77	10000
IKK-epsilon	86	10000
INSR	85	10000
INSRR	98	10000
IRAK1	82	10000
IRAK3	100	10000
IRAK4	92	10000
ITK	95	10000
JAK1(JH1domain-catalytic)	100	10000
JAK1(JH2domain-pseudokinase)	69	10000
JAK2(JH1domain-catalytic)	93	10000
JAK3(JH1domain-catalytic)	100	10000
JNK1	70	10000
JNK2	90	10000
JNK3	88	10000
KIT	92	10000
KIT(A829P)	94	10000
KIT(D816H)	90	10000
KIT(D816V)	92	10000
KIT(L576P)	96	10000
KIT(V559D)	91	10000
KIT(V559D,T670I)	86	10000
KIT(V559D,V654A)	96	10000
KIT-autoinhibited	71	10000
LATS1	95	10000
LATS2	91	10000
LCK	87	10000
LIMK1	77	10000
LIMK2	62	10000
LKB1	81	10000
LOK	96	10000
LRRK2	86	10000
LRRK2(G2019S)	100	10000
LTK	90	10000
LYN	86	10000
LZK	92	10000
MAK	98	10000
MAP3K1	87	10000
MAP3K15	76	10000

MAP3K2	100	10000
MAP3K3	73	10000
MAP3K4	99	10000
MAP4K2	94	10000
MAP4K3	100	10000
MAP4K4	90	10000
MAP4K5	92	10000
MAPKAPK2	84	10000
MAPKAPK5	73	10000
MARK1	93	10000
MARK2	66	10000
MARK3	67	10000
MARK4	91	10000
MAST1	87	10000
MEK1	82	10000
MEK2	69	10000
MEK3	85	10000
MEK4	92	10000
MEK5	83	10000
MEK6	98	10000
MELK	98	10000
MERTK	100	10000
MET	90	10000
MET(M1250T)	96	10000
MET(Y1235D)	100	10000
MINK	77	10000
MKK7	97	10000
MKNK1	89	10000
MKNK2	94	10000
MLCK	93	10000
MLK1	94	10000
MLK2	79	10000
MLK3	94	10000
MRCKA	97	10000
MRCKB	100	10000
MST1	83	10000
MST1R	93	10000
MST2	97	10000
MST3	70	10000
MST4	85	10000
MTOR	99	10000
MUSK	98	10000

MYLK	94	10000
MYLK2	100	10000
MYLK4	87	10000
MYO3A	89	10000
MYO3B	97	10000
NDR1	90	10000
NDR2	93	10000
NEK1	100	10000
NEK10	92	10000
NEK11	99	10000
NEK2	95	10000
NEK3	76	10000
NEK4	86	10000
NEK5	87	10000
NEK6	90	10000
NEK7	92	10000
NEK9	92	10000
NIK	95	10000
NIM1	96	10000
NLK	100	10000
OSR1	85	10000
p38-alpha	93	10000
p38-beta	96	10000
p38-delta	92	10000
p38-gamma	77	10000
PAK1	96	10000
PAK2	96	10000
PAK3	92	10000
PAK4	85	10000
PAK6	97	10000
PAK7	96	10000
PCK1	85	10000
PCK2	93	10000
PCK3	97	10000
PDGFRA	88	10000
PDGFRB	91	10000
PDPK1	95	10000
PFCDPK1(P.falciparum)	87	10000
PFPK5(P.falciparum)	100	10000
PFTAIRE2	94	10000
PFTK1	95	10000
PHKG1	100	10000

PHKG2	79	10000
PIK3C2B	98	10000
PIK3C2G	92	10000
PIK3CA	100	10000
PIK3CA(C420R)	77	10000
PIK3CA(E542K)	76	10000
PIK3CA(E545A)	81	10000
PIK3CA(E545K)	67	10000
PIK3CA(H1047L)	98	10000
PIK3CA(H1047Y)	75	10000
PIK3CA(I800L)	65	10000
PIK3CA(M1043I)	91	10000
PIK3CA(Q546K)	85	10000
PIK3CB	100	10000
PIK3CD	83	10000
PIK3CG	88	10000
PIK4CB	99	10000
PIM1	86	10000
PIM2	89	10000
PIM3	100	10000
PIP5K1A	100	10000
PIP5K1C	99	10000
PIP5K2B	100	10000
PIP5K2C	83	10000
PKAC-alpha	95	10000
PKAC-beta	95	10000
PKMYT1	100	10000
PKN1	81	10000
PKN2	98	10000
PKNB(M.tuberculosis)	78	10000
PLK1	91	10000
PLK2	67	10000
PLK3	77	10000
PLK4	87	10000
PRKCD	85	10000
PRKCE	100	10000
PRKCH	98	10000
PRKCI	72	10000
PRKCQ	91	10000
PRKD1	93	10000
PRKD2	95	10000
PRKD3	89	10000

PRKG1	100	10000
PRKG2	78	10000
PRKR	100	10000
PRKX	100	10000
PRP4	100	10000
PYK2	94	10000
QSK	83	10000
RAF1	99	10000
RET	87	10000
RET(M918T)	96	10000
RET(V804L)	99	10000
RET(V804M)	100	10000
RIOK1	100	10000
RIOK2	94	10000
RIOK3	100	10000
RIPK1	0	10000
RIPK2	98	10000
RIPK4	83	10000
RIPK5	68	10000
ROCK1	94	10000
ROCK2	100	10000
ROS1	85	10000
RPS6KA4(Kin.Dom.1-N-terminal)	97	10000
RPS6KA4(Kin.Dom.2-C-terminal)	99	10000
RPS6KA5(Kin.Dom.1-N-terminal)	96	10000
RPS6KA5(Kin.Dom.2-C-terminal)	80	10000
RSK1(Kin.Dom.1-N-terminal)	89	10000
RSK1(Kin.Dom.2-C-terminal)	80	10000
RSK2(Kin.Dom.1-N-terminal)	93	10000
RSK2(Kin.Dom.2-C-terminal)	100	10000
RSK3(Kin.Dom.1-N-terminal)	83	10000
RSK3(Kin.Dom.2-C-terminal)	65	10000
RSK4(Kin.Dom.1-N-terminal)	100	10000
RSK4(Kin.Dom.2-C-terminal)	61	10000
S6K1	80	10000
SBK1	80	10000
SGK	81	10000
SgK110	100	10000
SGK2	88	10000
SGK3	84	10000
SIK	96	10000
SIK2	91	10000

SLK	83	10000
SNARK	92	10000
SNRK	80	10000
SRC	94	10000
SRMS	75	10000
SRPK1	86	10000
SRPK2	90	10000
SRPK3	87	10000
STK16	100	10000
STK33	71	10000
STK35	96	10000
STK36	91	10000
STK39	88	10000
SYK	66	10000
TAK1	76	10000
TAOK1	98	10000
TAOK2	70	10000
TAOK3	88	10000
TBK1	89	10000
TEC	100	10000
TESK1	96	10000
TGFBR1	94	10000
TGFBR2	94	10000
TIE1	100	10000
TIE2	98	10000
TLK1	85	10000
TLK2	100	10000
TNIK	93	10000
TNK1	76	10000
TNK2	86	10000
TNNI3K	100	10000
TRKA	100	10000
TRKB	89	10000
TRKC	97	10000
TRPM6	87	10000
TSSK1B	83	10000
TTK	53	10000
TXK	93	10000
TYK2(JH1domain-catalytic)	100	10000
TYK2(JH2domain-pseudokinase)	78	10000
TYRO3	94	10000
ULK1	96	10000

ULK2	88	10000
ULK3	79	10000
VEGFR2	94	10000
VRK2	76	10000
WEE1	90	10000
WEE2	95	10000
WNK1	89	10000
WNK3	96	10000
YANK1	82	10000
YANK2	88	10000
YANK3	87	10000
YES	88	10000
YSK1	100	10000
YSK4	97	10000
ZAK	93	10000
ZAP70	99	10000

Inhibition of human, monkey, rabbit, rat, dog, mouse, and minipig RIP1 activity in the fluorescence polarization (FP) assay

Compound **6** was tested against six nonhuman species of RIP1 in FP binding assays using the method described in Harris et al. (2016). The mean IC₅₀ from a minimum of duplicate determinations is summarized in Table S4. Values for human and monkey RIP1 are at the lower limit of sensitivity (ca. 10 nM). Using the tight binding potency of 6.3 nM reported in Table 1 the species selectivity is underestimated by ca. 3 fold (e.g., rabbit is 380-fold less potent than human).

Table S4. RIP1 Species Selectivity of Compound **6**.

Species	RIP1 FP IC ₅₀ (μM)	Fold
Human	0.016	1
Monkey	0.026	1.6
Rabbit	2.4	150
Rat	>3.1	>190
Dog	7.1	440
Mouse	>10	>625
Mini Pig	>10	>625

7. Compound 6 RIP1 co-crystallization

Methods:

Crystals of the RIP1 complex with benzazepinone **6** were obtained by co-crystallization using sitting drop vapor diffusion with all sample manipulation carried out at 4°C or over ice. 100nL drops of the protein at 14.8mg/ml in the storage buffer (25mM Tris-HCl, 150mM NaCl, 1mM DTT, 10% glycerol, pH7.5) with 4mM benzazepinone **6** (dissolved in DMSO) were dispensed using a Mosquito dispensing robot into a 96 well plate and incubated against the Qiagen PEGS I crystallization screening kit from which 150nL was dispensed on top of the protein drop. Crystals were obtained from solution 34 (100mM MES pH 6.5, 25% PEG 8k) and grew to full size over approximately one week. Crystals were quickly transferred through a 10µL drop containing precipitant solution, 10% ethylene glycol and 4mM benzazepinone **6** before plunge freezing into liquid nitrogen.

Data was collected at the ESRF synchrotron in Grenoble, France on beamline ID29 using a Pilatus 6M detector where 180° of data was collected using a oscillation increment of 0.2°. Data processing was carried out using the synchrotrons implementation of the Global Phasing program autoPROC (Acta Cryst. D67, 293-302 (2011)).

Structure determination was done by molecular replacement using the atomic coordinates of RIP1 kinase domain with Necrostatin-4 (PDB code 4ITJ) as a search model.

Refinement was carried out with the Global Phasing program Buster (Acta Cryst. D68, 368-380 (2012)) with a previously solved but undisclosed higher resolution target structure utilized for structural restraints. The chemical library for benzazepinone **6** was generated with phenix.elbow (Acta Cryst. D66, 213-221 (2010)) modified by the Cambridge Crystallographic Data Centre program Mogul. All model building was carried out with COOT (Acta Cryst D66, 486-501, 2010) and figures generated utilizing the CCP4 program CCP4MG (Acta Cryst. D67, 386-394 (2011)).

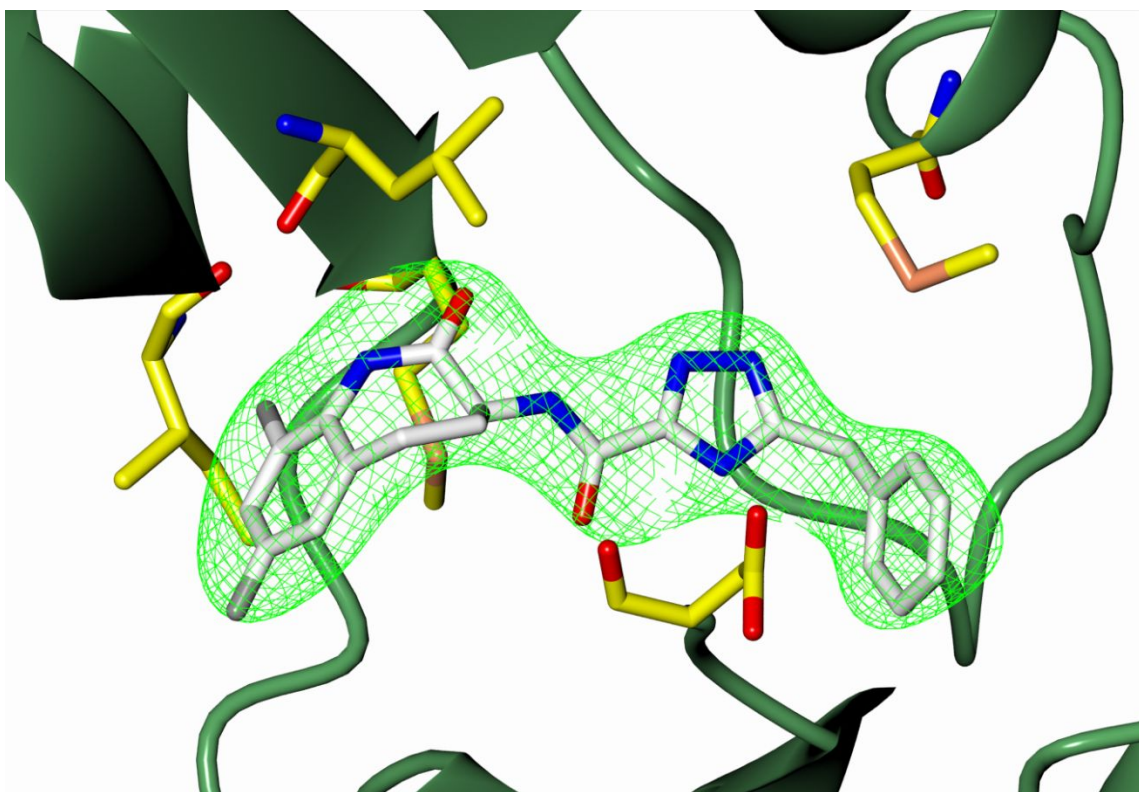
Coordinates and structure factors for the cocrystal structure of RIP1 (1–294, C34A, C127A, C233A, C240A) and benzoxazepinone **6** have been deposited in the Protein Data Bank with the accession number 6RLN.

Table S5: X-ray diffraction processing and refinement statistics for the RIP1 benzazepinone **6** complex structure.

	Overall	Innershell	Outershell
Low Res Limit (Å)	48.83	48.83	2.97
High Res Limit (Å)	2.87	11.12	2.87
Rmerge (all)	0.064	0.028	1.188
Mean(I/σI)	17.6	50.9	1.5
Observations (unique)	99490 (15475)	1651 (325)	9183 (1420)

Completeness	99.4	98.8	95.3
Multiplicity	6.4	5.1	6.5
Space Group	P212121		
Unit Cell Dimensions	101.840	130.790	48.830 90.00 90.00 90.00
R-factor (R-Free)	0.1939 (0.2318)		

Figure S4: The binding orientation of benzazepinone **6** in the active site pocket of RIP1 produced by single crystal X-ray crystallography with associated omit map electron density contoured at 3σ and a resolution of 2.87\AA .

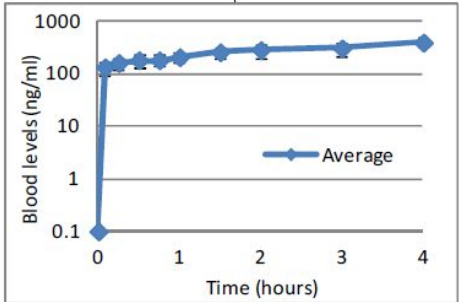


8. Compound 6: rat tissue distribution, permeability and p-gp substrate evaluation, hepatocyte turnover, metabolite ID and human PK/PD prediction.

Tissue Distribution of compound **6** in the male Han Wistar rat via constant intravenous infusion over 4 hours at a dose of 2.3 mg/kg (dosed in 20% Cavitron; 5% DMSO at dose volume of 4 mL/kg). At the end of the infusion, animals were euthanized and tissues were collected (brain, heart, kidney, liver, colon, skin and eyes). Homogenates were prepared in acetonitrile. Tissue homogenate concentrations were

determined based on a standard curve prepared in an identical fashion to the study animal tissue homogenates, using a tissue specimen from an untreated control rat. The tissue-to-blood ratio for each compound was calculated by dividing tissue concentration (expressed as ng compound/g tissue) by the approximate steady-state blood concentration (Table S6).

Table S6. Tissue distribution of compound **6**

2.3 mg/kg (4 hour infusion)	Conc at 4h (ng/mL)	Tissue	Tissue Concentration (ng/g tissue)	Tissue:Blood ratio [ng/g tissue]: [ng/mL]
	395 ± 98	Brain	24 ± 4	0.06 ± 0.01
	Kidney	3300 ± 560	8.4 ± 1.4	
	Heart	1200 ± 170	3.1 ± 0.4	
	Liver	3000 ± 240	7.6 ± 0.6	
	Colon	1100 ± 600	2.8 ± 1.6	
	Eye	92 ± 18	0.23 ± 0.05	
	Skin	290 ± 90	0.73 ± 0.23	

Compound **6** was evaluated for permeability across MDR1-MDCK cell monolayers with and without the P-gp inhibitor cyclosporin A (CSA). P-gp substrate is classified as positive if the efflux ratio > 3.0 in the absence of inhibitor and ~1 in the presence of inhibitor (Table S7).

Table S7. MDCK permeability of compound **6**

Cell Line	Treatment	Papp (nm/s)		Efflux Ratio
		A-B	B-A	B-A/A-B
MDR1-MDCK	Compound 6	3.4	386	115
	Compound 6 + PgP Inhibitor	67.4	58.5	0.90

In vitro evaluation of metabolic stability of compound **6** in the presence of NADPH, indicated moderate turnover in the rat and low turnover in both monkey and human hepatocytes as shown Table S8.

Table S8. Hepatocyte turnover of compound **6**. Human hepatocytes were from mixed gender, whereas rat and monkey were from male only.

Species	Rat	Monkey	Human
Hepatocyte Clearance (mL/min/g Liver)	1.9	<0.50	<0.50

Allometric scaling and in vitro to in vivo extrapolations with and with-out effects of free fraction were used to generate predictions of human PK parameters (Table S9).

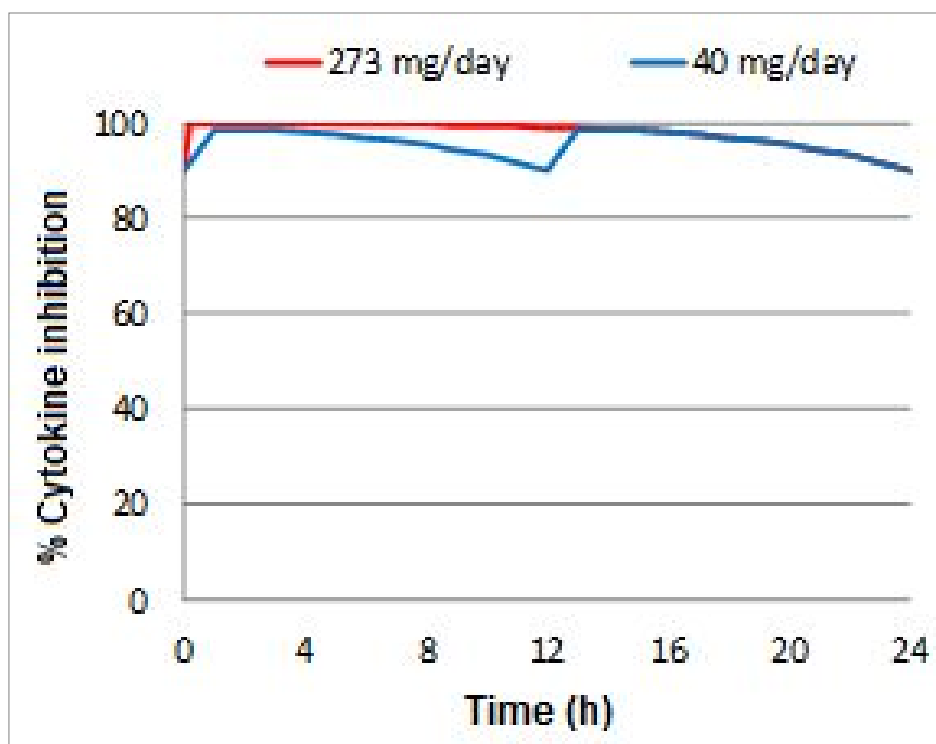
Table S9. Average predicted human PK profile of **6** based on PK Predictor Pro software.

Parameter	Average	+95%	-95%
Clearance (mL/min/kg)	4.6	5.8	3.4
Volume (L/kg)	1.3	1.5	1.1
<u>Half life</u> (h)*	3-3		
Bioavailability (%)	83	87	79

* Half-life based on reconstructed PK profiles.

The predicted human PK/PD was modelled using the predicted human PK profile along with human whole blood activity as shown in Figure S5.

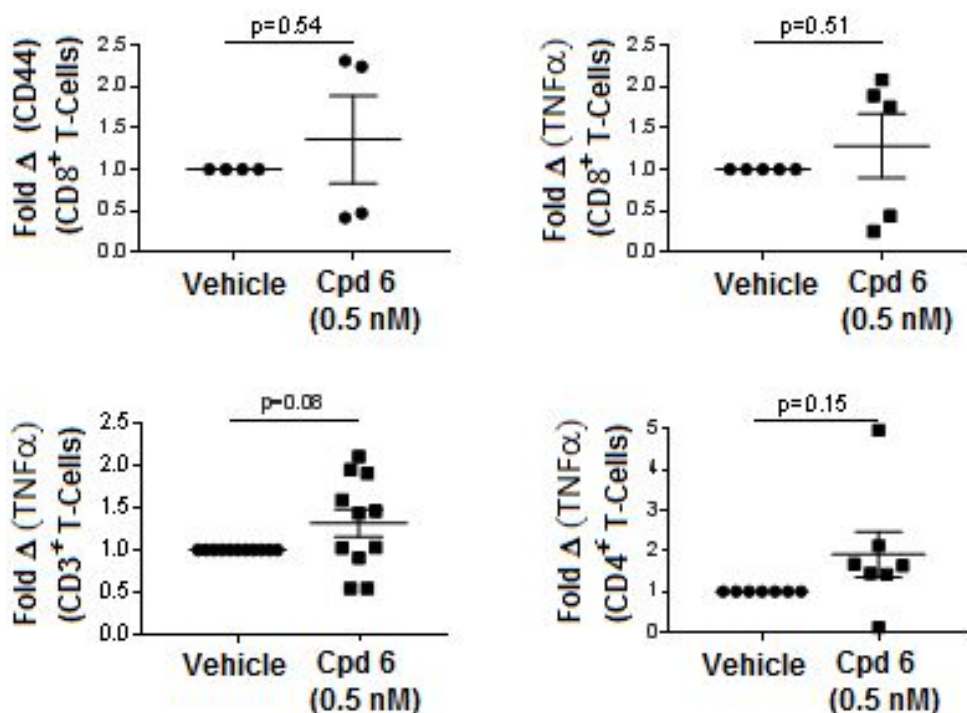
Figure S5. Predicted human PD dose effect levels of benzaepinone **6** at 273 mg once daily and 40 mg twice daily, maintaining 90% RIP1 inhibition levels over 24 hours.



9. Additional PDOTS evaluation.

PDOTS prepared from tumors from pancreatic adenocarcinoma, colorectal, breast and gastric cancer patients treated with compound **6** show a trend toward increased effector-memory CD8⁺ T cells and TNF α expression, although these markers failed to reach statistical significance in this study (Figure S6). Compound **6** was dissolved to a concentration of 10 μ M in DMSO and underwent 1:200 dilution in culture medium to a final concentration of 0.5 nM. Vehicle control was a similar 0.5% DMSO solution in culture medium.

Figure S6. PDOTS prepared from tumors from pancreatic adenocarcinoma, colorectal, breast and gastric cancer patients treated with compound **6**.



10. References

Adams, P. D.; Afonine, P. V.; Bunkoczi, G.; Chen, V. B.; Davis, I. W.; Echols, N.; Headd, J. J.; Hung, L. W.; Kapral, G. J.; Grosse-Kunstleve, R. W.; McCoy, A. J.; Moriarty, N. W.; Oeffner, R.; Read, R. J.; Richardson, D. C.; Richardson, J. S.; Terwilliger, T. C.; Zwart, P. H. PHENIX: a comprehensive Python-based system for macromolecular structure solution. *Acta Crystallogr. D. Biol Crystallogr.* **2010**, *66*, 213-221.

Bricogne, G. BUSTER. **2013**. Cambridge, UK, Global Phasing Ltd. (Computer Program)

Degterev, A.; Hitomi, J.; Gemscheid, M.; Ch'en, I. L.; Korkina, O.; Teng, X.; Abbott, D.; Cuny, G. D.; Yuan, C.; Wagner, G.; Hedrick, S. M.; Gerber, S. A.; Lugovskoy, A.; Yuan, J. Identification of RIP1 kinase as a specific cellular target of necrostatins. *Nat. Chem. Biol.* **2008**, *4*, 313-321.

Fabian M. A., Biggs W H 3rd, Treiber D K, Atteridge C E, Azimioara M D, Benedetti M G, Carter T A, Ciceri P, Edeen P T, Floyd M, Ford J M, Galvin M, Gerlach J L, Grotzfeld R M, Herrgard S, Insko D E, Insko M A, Lai A G, Lélías J M, Mehta S A, Milanov Z V, Velasco A M, Wodicka L M, Patel H K, Zarrinkar P P, Lockhart D J. A small molecule-kinase interaction map for clinical kinase inhibitors. *Nat. Biotechnol.* **2005**, *23*, 329-336.

Harris, P. A.; Bandyopadhyay, D.; Berger, S. B.; Campobasso, N.; Capriotti, C. A.; Cox, J. A.; Dare, L.; Finger, J. N.; Hoffman, S. J.; Kahler, K. M.; Lehr, R.; Lich, J. D.; Nagilla, R.; Nolte, R. T.; Ouellette, M. T.; Pao, C. S.; Schaeffer, M. C.; Smallwood, A.; Sun, H. H.; Swift, B. A.; Totoritis, R. D.; Ward, P.; Marquis, R. W.; Bertin, J.; Gough, P. J. Discovery of Small Molecule RIP1 Kinase Inhibitors for the Treatment of Pathologies Associated with Necroptosis. *ACS Med. Chem. Lett.* **2013**, *4*, 1238-1243.

Harris, P. A.; King, B. W.; Bandyopadhyay, D.; Berger, S. B.; Campobasso, N.; Capriotti, C. A.; Cox, J. A.; Dare, L.; Dong, X.; Finger, J. N.; Grady, L. C.; Hoffman, S. J.; Jeong, J. U.; Kang, J.; Kasparcova, V.; Lakdawala, A. S.; Lehr, R.; McNulty, D.E.; Nagilla, R.; Ouellette, M. T.; Pao, C. S.; Rendina, A. R.; Schaeffer, M. C.; Summerfield, J. D.; Swift, B.A.; Totoritis, R.D.; Ward, P.; Zhang, A.; Zhang, D.; Marquis, R. W.; Bertin, J.; Gough, P. J. DNA-Encoded Library Screening Identifies Benzo[b][1,4]oxazepin-4-ones as Highly Potent and Monoselective Receptor Interacting Protein 1 Kinase Inhibitors. *J. Med. Chem.* **2016**, *59*, 2163-2178.

Jameson, D. M., Mocz, G. *Methods Mol. Biol.* (Totowa, NJ, U.S.) **2005**, 305, 301

Kabsch, W. *XDS. Acta Cryst.* **2010**, *D66*, 125-132.

Kestranek, A., Chervenak, A., Longenberger, J., Placko, S. Chemiluminescent nitrogen detection (CLND) to measure kinetic aqueous solubility. *Curr Protoc Chem Biol.* **2013**, *5*, 269-280.

Li, L.; Thomas, R. M.; Suzuki, H.; De Brabander, J. K.; Wang, X.; Harran, P. G. A Small Molecule Smac Mimic Potentiates TRAIL and TNF α -mediated Cell Death. *Science* **2004**, *305*, 1471–1474.

Tummino, P.J., Copeland, R.A. Residence Time of Receptor-Ligand Complexes and Its Effect on Biological Function. *Biochemistry* **2008**, *47*, 5481-5492.

Valkó, K. Chromatographic hydrophobicity index by fast-gradient RP-HPLC: a high-throughput alternative to log P/log D. *Anal. Chem.* **1997**, *69*, 2022–2029.

Wasilko D., Lee S.E. TIPS: Titerless Infected Cells Preservation and Scale up. *BioProcessing.* **2006**, Fall, 2-32.

Williams, W.W., Morrison, J.F. The Kinetics of Reversible Tight-Binding Inhibition. *Meth. Enzymol.* **1979**, *63*, 437-467.

Winn, M. D., Ballard, C. C., Cowtan, K. D., Dodson, E. J., Emsley, P., Evans, P. R., Keegan, R. M., Krissinel, E. B., Leslie, A. G. W., McCoy, A. McNicholas, S. J., Murshudov, G. N., Pannu, N. S., Potterton, E. A., Powell, H. R., Read, R. J., Vagin A., Wilson K. S. Overview of the CCP4 suite and current developments *Acta. Cryst.* **2011**, *D67*, 235-242.

Xie, T.; Peng, W.; Liu, Y.; Yan, C.; Maki, J.; Degtarev, A.; Yuan, J.; Shi, Y. Structural basis of RIP1 inhibition by necrostatins. *Structure* **2013**, *21*, 493-499.